Published in final edited form as:
J Comp Neurol. 2013 August 1; 521(11): 2486–2501. doi:10.1002/cne.23294.

Expression of Voltage-Gated Calcium Channel $\alpha_2\delta_4$ Subunits in the Mouse and Rat Retina

Luis Pérez De Sevilla Müller[1,*], **Janelle Liu**[1], **Alexander Solomon**[1], **Allen Rodriguez**[1], and **Nicholas C. Brecha**[1,2,3,4,5]

[1]Department of Neurobiology, David Geffen School of Medicine at UCLA, University of California, Los Angeles, California 90095

[2]Department of Medicine, David Geffen School of Medicine at UCLA, University of California, Los Angeles, California 90095

[3]Jules Stein Eye Institute, David Geffen School of Medicine at UCLA, University of California, Los Angeles, California 90095

[4]CURE-Digestive Diseases Research Center, David Geffen School of Medicine at UCLA, University of California, Los Angeles, California 90095

[5]Veterans Administration Greater Los Angeles Healthcare System, Los Angeles, California 90073

Abstract

High-voltage activated Ca channels participate in multiple cellular functions, including transmitter release, excitation, and gene transcription. Ca channels are heteromeric proteins consisting of a pore-forming α_1 subunit and auxiliary $\alpha_2\delta$ and β subunits. Although there are reports of $\alpha_2\delta_4$ subunit mRNA in the mouse retina and localization of the $\alpha_2\delta_4$ subunit immunoreactivity to salamander photoreceptor terminals, there is a limited overall understanding of its expression and localization in the retina. $\alpha_2\delta_4$ subunit expression and distribution in the mouse and rat retina were evaluated by using reverse transcriptase polymerase chain reaction, western blot, and immunohistochemistry with specific primers and a well-characterized antibody to the $\alpha_2\delta_4$ subunit. $\alpha_2\delta_4$ subunit mRNA and protein are present in mouse and rat retina, brain, and liver homogenates. Immunostaining for the $\alpha_2\delta_4$ subunit is mainly localized to Müller cell processes and endfeet, photoreceptor terminals, and photoreceptor outer segments. This subunit is also expressed in a few displaced ganglion cells and bipolar cell dendrites. These findings suggest that the $\alpha_2\delta_4$ subunit participates in the modulation of L-type Ca^{2+} current regulating neurotransmitter release from photoreceptor terminals and Ca^{2+}-dependent signaling pathways in bipolar and Müller cells.

INDEXING TERMS

calcium channel; $\alpha_2\delta_4$ subunit; Müller cell; photoreceptor; retina; mouse; rat

*CORRESPONDENCE TO: Luis Pérez De Sevilla Müller, Ph. D., Department of Neurobiology, David Geffen School of Medicine at Los Angeles, University of California, Los Angeles, 10833 Le Conte Ave., Los Angeles, CA 90095-1763. luisperez@mednet.ucla.edu.

CONFLICT OF INTEREST STATEMENT
The authors have no conflict of interest.

Voltage-gated Ca channels are transmembrane, multimeric proteins that mediate numerous neuronal functions, including transmitter release, gene transcription, and synaptic plasticity (reviewed in Catterall, 2000). Voltage-gated Ca channels are classified into two major groups based on their electrophysiological and pharmacological properties; 1) low voltage-activated (LVA) Ca channels that are characterized by three T-type channels; and 2) high voltage-activated (HVA) Ca channels that are characterized by L-, N-, P/Q-. and R-type channels. Structurally, Ca channels consist of a single, pore-forming and voltage-sensing α_1 subunit together with auxiliary $\alpha_2\delta$ and β subunits. In mammals, four genes (Cacna2d1–4) encode the $\alpha_2\delta$ family: $\alpha_2\delta_1$–$\alpha_2\delta_4$ (Catterall, 2000). The $\alpha_2\delta$ subunits enhance Ca channel expression and trafficking, and also affect the biophysical properties of Ca channels (reviewed in Davies et al., 2007; Bauer et al., 2010; Dolphin, 2012). However, there are questions remaining regarding the cellular and tissue distribution of the $\alpha_2\delta$ subunits, and, in addition, the specific association between the subtypes of α_1 and $\alpha_2\delta$ subunits is poorly understood (for reviews, see Davies et al., 2007; Dolphin, 2012).

$\alpha_2\delta_{1–2}$ subunit mRNAs are found in multiple tissues, including the nervous system, heart, and other internal organs (Klugbauer et al., 1999; Gao et al., 2000; Barclay et al., 2001; Brodbeck et al., 2002; Gong et al., 2001; Cole et al., 2005), whereas $\alpha_2\delta_3$ subunit mRNA and protein are reported to be exclusively expressed in the brain (Klugbauer et al., 1999; Gao et al., 2000; Gong et al., 2001). $\alpha_2\delta_4$ subunit mRNA has been previously reported to be absent in the human and mouse brain (Qin et al., 2002; Schlick et al., 2010). Recently, this subunit has been reported to be associated with the α_{1F} subunit near ribbon synapses at the base of photoreceptors in the salamander retina (Mercer et al., 2011). Consistent with the expression of $\alpha_2\delta_4$ subunit in the retina are findings of a novel outer retinal disease in a substrain of C57BL/10 mice having a mutation in the Cacna2d4 gene (Ruether et al., 2000; Wycisk et al., 2006a,b). In this mutant, there are alterations of the electroretinogram (ERG), including reduction of the b-wave and absence of a photopic ERG. There are also morphological changes, including loss of ribbon synapses in rod photoreceptor spherules, and an altered structure of cone photoreceptor pedicles. It is unknown whether the $\alpha_2\delta_4$ subunit directly mediates these electrophysiological and morphological changes or whether the subunit affects cellular processes that participate in the formation and function of ribbon synapses.

We report the mRNA expression and protein localization of the $\alpha_2\delta_4$ subunit in the mouse and rat retina by using reverse transcriptase polymerase chain reaction (RT-PCR), western blotting, and immunocytochemistry. $\alpha_2\delta_4$ subunit mRNAs and protein are in the retina, brain, and liver of the mouse and rat. $\alpha_2\delta_4$ immunostaining is observed in retinal Mu¨ller cells and in some neurons in the inner nuclear layer (INL). In the rat retina, a diffuse band of immunoreactivity was found in the outer plexi-form layer (OPL), whereas in the mouse retina, prominent immunoreactive puncta were found at the base of photoreceptor terminals. Double-labeling studies of wild-type and transgenic mouse retinas with $\alpha_2\delta_4$ subunit antibodies and specific retinal cell markers showed that this sub-unit is located in Müller cells, displaced ganglion cells, bipolar cell dendrites, and photoreceptors. The localization of the $\alpha_2\delta_4$ subunit suggests that this subunit participates in Ca channel-mediated processes, including neurotransmission at photoreceptor terminals, and modulation of Ca signaling in Müller cells.

MATERIALS AND METHODS

Animal preparation

Animal care and all experiments were carried out in accordance with the guidelines for the welfare of experimental animals issued by the U.S. Public Health Service Policy on Human Care and Use of Laboratory Animals (2002) and the University of California at Los Angeles

(UCLA) Chancellor's Animal Research Committee. Adult Sprague-Dawley rats (250–300 g, >1 month old), wild-type C57BL/6 (20–30 g; <3 months old; The Jackson Laboratory, Bar Harbor, ME), rd mice (Carter-Dawson et al., 1978; <2 months old), and cone-diphtheria toxin A (DTA) mice (Soucy et al., 1998; ~1 year old) of both sexes were used for these studies. In addition, we crossed two transgenic mouse lines (B6;129P2-Pvalb$^{tm1(cre)Arbr}$/J (PV-cre) and B6.Cg-Gt(ROSA)26Sor^{tm14} (CAG-tdTomato)Hze/J (ROSA26-tdTomato)) obtained from The Jackson Laboratory. PV-cre expresses Cre recombinase from the endogenous Pvalb, or parvalbumin, locus. When crossed with the ROSA26-tdTomato line, the resulting offspring have the STOP cassette deleted in the cre-expressing tissue, resulting in expression of the fluorescent protein tdTomato. These mice express tdTomato in a subset of ganglion cells of the ganglion cell layer (GCL) and some displaced ganglion cells (Haverkamp et al., 2009; Munch et al., 2009).

Mice and rats were deeply anesthetized with 1–3% iso-fluorane (IsoFlo, Abbott Laboratories, North Chicago, IL), and subsequently killed by cervical dislocation or decapitation by using a guillotine. The eyes were removed and dissected in Hibernate A, a CO_2-independent nutrient medium for the maintenance of neural cells, tissue, and tissue slices (Invitrogen, Carlsbad, CA). All dissections were performed in the afternoon (2–4 PM) at a light intensity of 3.2×10^3 lux. Mouse and rat eyecups were fixed in 4% paraformaldehyde (PFA) in 0.1 M phosphate buffer (PB), pH 7.4, for 15–60 minutes at room temperature, washed in 0.1 M PB, and stored in 30% sucrose in PB overnight at 4°C. Eyecups were embedded in optimal cutting temperature (O.C.T.) medium (Sakura Finetek, Torrance, CA) and sectioned vertically at 12–14 μm onto gelatin-coated slides by using a Leica CM3050S cryostat (Leica Microsystems, Buffalo Grove, IL).

Immunohistochemistry

Retinal sections were incubated with 3–5% normal goat sera with 0.3% Triton X-100 in 0.1 M PB for 1–2 hours at room temperature. After the blocking procedure, primary antibodies (see Table 1) were added and incubated overnight at 4°C in a humidified chamber. The sections were washed 3 times for 10 minutes each in 0.1 M PB and the corresponding secondary antibody was applied for 2 hours at room temperature in the dark. Secondary antibodies used in this study were Alexa Fluor 488-, 594-, 568-, or 633-conjugated goat anti-rabbit, mouse, or rat IgG antibodies (Invitrogen) at 1:500–1:1,000 dilutions. After a final wash of 3 times 10 minutes in 0.1 M PB, the retinal sections were coverslipped in Vectashield (Vector, Burlingame, CA) or Aqua Poly/Mount mounting medium (Polysciences, Warrington, PA).

As a negative control, the omission of the primary antibodies in the single and double-labeling studies was conducted to control for nonspecific binding of the secondary antibody. To evaluate the specificity of the primary antibody immunostaining, a preadsorption control was performed. Briefly, the $\alpha_2\delta_4$ subunit antibody was diluted in 0.1 M PB containing 0.3% Triton X-100 and mixed with the corresponding Protein Epitope Signature Tag (PrEST) antigen (Atlas Antibodies, Stockholm, Sweden) of human Cacna2d4 at a final concentration of 1 lg/ml for 1–12 hours at room temperature. This antigen is fused to a dual tag consisting of the His6 tag and albumin-binding protein. The antibodies directed against this dual tag are thoroughly depleted before capturing the antigen (Cacna2d4)-specific antibodies in a separate purification step. No immunostaining was present in sections incubated with the preabsorbed $\alpha_2\delta_4$ subunit antibody, showing the specificity of the antibody (see Results).

Antibody characterization

A polyclonal rabbit antibody (cat. #HPA031952; Sigma, St. Louis, MO) to the human $\alpha_2\delta_4$ peptide sequence above was used to detect $\alpha_2\delta_4$ subunit immunoreactivity. The antibody

was characterized by western blot analysis (Fig. 1). The antibody detected a 170 kDa protein band, corresponding to the apparent molecular mass of the $\alpha_2\delta_4$ subunit under nonreducing conditions (Davies et al., 2007). Specificity of the $\alpha_2\delta_4$ subunit antibody was also demonstrated in the mouse and rat retina in sections incubated in the primary antibody preabsorbed with the $\alpha_2\delta_4$ PrEST antigen. Immunostaining was absent in these sections (see Results).

The mouse monoclonal antibody against the bassoon protein (cat. #SAP7F407; Enzo Life Sciences, Farmingdale, NY) detected a 400 kDa band in a western blot of the mouse and rat brain (manufacturer's data sheet). The bassoon monoclonal antibody is a well-established marker for photoreceptor ribbons, and no immunostaining is detected in bassoon knockout (KO) retinas (Brandstätter et al., 1999; Dick et al., 2003).

The mouse monoclonal antibody against the C-terminal binding protein 2 (CtBP2) (cat. #612044; BD Biosciences, San Jose, CA) detected a 48 kDa band in a western blot of rat brain membrane fractions (tom Dieck et al., 1998). This monoclonal antibody recognizes synaptic ribbons in photoreceptors and bipolar cells of mouse, cow, and monkey retinas (Schmitz et al., 2000; tom Dieck et al., 2005; Jusuf et al., 2006; Puller et al., 2007).

The mouse monoclonal antibody to glutamic acid decarboxylase 65 (GAD_{65}) (cat. #MAB351; Millipore, Temecula, CA) detected a single band at 59 kDa (Erlander et al., 1991) in western blots of unfractionated homogenates of whole rat brain (Chang and Gottlieb, 1988). In addition, the band was absent in homogenates of brain from GAD_{65} KO mice (Yamamoto et al., 2004). This GAD_{65} antibody immunostains amacrine and displaced amacrine cells in the mouse and rat retina (Brecha et al., 1991; Haverkamp and Wässle, 2000).

The mouse monoclonal antibody to GAD_{67} (cat. #MAB5406; Millipore) detected a single band at 67 kDa (Erlander et al., 1991) in western blots of rat cortex and does not cross-react with the GAD_{65} isoform in a western blot of rat cortex (Fong et al., 2005). In addition, immunostaining in the brain was reduced in a conditional GAD_{67} KO mutant (Heusner et al., 2008).

The mouse monoclonal antibody to glutamine synthetase (GS) (cat. #610518, BD Biosciences) detected a single band of 45 kDa in western blots of rat brain (manufacturer's data sheet). This antibody produced specific immunostaining of Müller cells in the mouse retina (Linser et al., 1984; Zhang et al., 2005).

The rat polyclonal antibody to glycine (cat. #IG1002, ImmunoSolution, Queensland, Australia) was tested by preabsorption with a PFA conjugate of glycine and thyroglobulin (Pow et al., 1995). Specificity was demonstrated by using immunoblotting against the same amino acid-PFA-thyroglobulin conjugate used to immunize the animals. The glycine polyclonal antibody also recognized dot blots containing glycine, but not related amino acids (Pow et al., 1995). This antibody selectively immunostains amacrine cells in the retina of multiple species, including mouse and rat (Pow and Hendrickson, 1999; Haverkamp and Wässle, 2000).

The mouse monoclonal antibody to Goα (cat. #MAB3073; Millipore) detected a single band of 42–43 kDa in homogenates of the olfactory epithelium and the vomeronasal organ in *Xenopus laevis* and *Bufo japonicas* (Hagino-Yamagishi and Nakazawa, 2011). In the retina, Goa is expressed in rod and cone ON-type bipolar cells (Haverkamp and Wässle, 2000; Dhingra et al., 2000).

The mouse monoclonal antibody to protein kinase C (PKC) (cat. #K01107M; Biodesign International, Saco, ME) was raised against PKC (79–80 kDa) purified from bovine brain. This antibody reacts with PKC-alpha/beta-1/beta-2 isoforms (manufacturer's data sheet). The PKC antibody recognized the purified PKC protein as well as an 80 kDa band from whole-cell extracts of rat glioma and murine NIH3T3 cell lines in Western blots and specifically immunoprecipitates PKC from cell lysates of 328 glioma and SVK 14 cell lines (Young et al., 1988). PKC is a specific marker for rod bipolar cells in the mouse and rat retina (Haverkamp and Wassle, 2000; Ghosh et al., 2001; Haverkamp et al., 2003). Immunostaining was completely blocked by the full-length peptide but was not blocked by an unrelated peptide (Young et al., 1988).

The mouse monoclonal antibody to postsynaptic density protein 95 (PSD-95) (cat. #MAB1596, Millipore) detected a single band at ~100 kDa, corresponding to the apparent molecular weight of PSD-95 on sodium dodecyl sulfate polyacrylamide gel electrophoresis (SDS-PAGE) immunoblots of rat, mouse, and bovine brain (manufacturer's data sheet). The antibody recognized a major band at ~95 kDa and a minor band at ~80 kDa on western blot of mouse and rat brain (manufacturer's data sheet). PSD-95 immunoreactivity is localized to photoreceptor terminals and postsynaptically to bipolar cell ribbon synapses in the inner plexiform layer (IPL) (Koulen at al., 1998).

The mouse monoclonal antibody to the vesicular c-aminobutyric acid (GABA) transporter (VGAT) (cat. #131 011; Synaptic Systems, Goettingen, Germany) recognizes a single band of the expected molecular size of 57 kDa (McIntire et al., 1997; Sagné et al., 1997) in western blots of mouse brain and retina (Guo et al., 2009). Preadsorption of this antibody with the VGAT N-terminus peptide used for immunization, $VGAT_{75–87}$ (AEPPVEGDIHYQR), eliminated the VGAT signal in a Western blot (manufacturer's data sheet) and abolished specific VGAT immunolabeling in mouse retina (Guo et al., 2009). This polyclonal antibody immunostains amacrine and displaced amacrine cells and their processes in the IPL, and horizontal cells and their endings in the OPL in mouse retina (Guo et al., 2009).

RT-PCR

Total RNA was extracted from retinal, cerebral cortex, and liver lysates of the mouse and rat by using the Absolutely RNA Miniprep Kit (Agilent Technologies, Santa Clara, CA) according to the manufacturer's instructions. RNA concentrations were determined spectrophotometrically with a DU530 Spectrophotometer (Beckman Coulter, Brea, CA). The isolated total RNA (1.0 μg) was used as a template for first-strand cDNA synthesis by using oligo(dT) to prime Superscript III First-Strand Synthesis System for RT-PCR, following the manufacturer's instructions (Invitrogen). PCR was performed with primers specific for two regions of the $\alpha_2\delta_4$ subunit transcript in mouse and rat. These primers recognize and amplify all three of the $\alpha_2\delta_4$ subunit variants known to exist in the mouse (Angelotti and Hoffman, 1996): (1) forward: 5'-ggagtcatcgccttcgactgc, reverse: 5'-agaaggcatagccatgcacc; and (2) forward: 5'-cactgatctcgactgcttcg, reverse: 5'-ttcttgtgcttgtgggagtg (Wycisk et al., 2006a). Primer set (1) corresponds to nucleotide positions 856–1,717 in rat and 925–1,786 in mouse, covering exons 7–16 of $\alpha_2\delta_4$ mRNA, whereas primer set (2) corresponds to nucleotide positions 2,706–3,062 in rat and positions 2,772–3,128 in mouse, spanning exons 28–35 (NCBI Reference Sequences: NM_001191751.1, NM_001033382.2). Fragment sizes for primer sets (1) and (2) are 862 bp and 357 bp, respectively.

PCR was performed in a 20-μl reaction volume containing 0.25 μM of each primer, 0.1 U/μl of EconoTaq DNA Polymerase, reaction buffer (pH 9.0), 400 μM dATP, 400 μM dGTP, 400 μM dCTP, 400 μM dTTP, 3 mM $MgCl_2$ (Lucigen, Middleton, WI), with 2 μl (1/10th) of the

cDNA synthesis reaction as template. The following temperature protocol was used: 2 minutes at 96°C, then 30 cycles of 30 seconds at 95°C, 30 seconds at 65°C or 70°C, 1 minute at 72°C, followed by a final extension of 5 minutes at 72°C. Then 5 μl of the PCR reaction was run out on a 1.5% agarose gel in 1XTAE (40 mM Tris-acetate, 1 mM EDTA buffer), and the DNA was visualized by using Gel Red (1:10,000) (Biotium, Hayward, CA).

Western blots

Rodent retina, cortex, and liver samples were isolated and placed immediately in 1.5 M Tris-HCl, 0.5 M EDTA, 0.5 M EGTA, and 20% Triton-X in dH_2O on dry ice. Six mouse and four rat retinas were used for each blot. Cell lysis buffer also contained 10 μl/ml Halt Protease Inhibitor and 10 μl/ml Halt Phosphatase Inhibitor cocktails (Thermo Fisher Scientific, Waltham, MA). Samples were homogenized for 2 minutes and incubated on ice for 20 minutes to lyse cells. After centrifugation (20,100g, 30 minutes at 4°C), the supernatant fractions were removed and the protein content of the samples was determined by using a Pierce BCA Protein Assay Kit (Thermo Fisher Scientific). Protein samples were diluted in Laemmli sample buffer without reducing agents, pH 6.8, and samples were boiled for 5 minutes before loading onto the gel.

Western blot analysis of the homogenates was performed after fractionating 35 μg of protein by 4–20% SDS-PAGE (200 V for 30 minutes) using Mini-PROTEAN TGX precast polyacrylamide gels (Bio-Rad, Hercules, CA). Prestained marker proteins were used as molecular mass standards (Bio-Rad). The separated proteins were transferred electrophoretically to PVDF Immobilon-FL membranes (Millipore) at 360 mA for 2 hours at 4°C. Blots were allowed to dry completely to increase protein retention before blocking with 5% nonfat dry milk in PBST for 45 minutes at room temperature and then rinsed in a solution containing 0.1 M PB, 0.154 M NaCl, and 0.05% Tween 20 (v/v) at pH 7.4. The blots were incubated for 1 hour at room temperature with the $\alpha_2\delta_4$ subunit antibody (see Table 1) at 1:200 in blocking buffer. In control strips, the primary antibody was omitted. Blots were washed and incubated in goat anti-rabbit IgG-conjugated IRDye 800CW (H + L) (LI-COR, Lincoln, NE) diluted at 1:10,000 in 3% dry milk in PBST for 1 hour at room temperature. The blots were washed and immediately imaged by using the LI-COR Odyssey Infrared Imaging System and evaluated by using proprietary software.

Fluorescent image acquisition and colocalization analysis

Immunostaining was examined by using a Zeiss Laser Scanning Microscope 510 Meta (Carl Zeiss, Thornwood, NY) with a Zeiss C-Apochromat 40×/1.2 NA corrected water objective, a Zeiss C-Apochromat 63×/1.2 NA corrected water objective, or a Zeiss Plan-Neofluar 63×/1.25 NA corrected oil objective at 2,048 × 2,048 pixels. Images are presented either as a single scan or as projections of three to five sections (z-axis step size 0.3–0.5 μm). Confocal images were analyzed by using the Zeiss LSM 510 proprietary software (version 3.2). The intensity levels and contrast of the final images were adjusted in Adobe Photoshop CS2 v. 9.02 (Adobe Systems, San Jose, CA).

RESULTS

Specificity and characterization of Ca channel $\alpha_2\delta_4$ subunit antibody

The presence of $\alpha_2\delta_4$ subunit mRNA and protein was tested in rat and wild-type mouse retina, brain, and liver by using RT-PCR and western blotting. RT-PCR yielded a single band of ~357 bp from the mouse and rat retina, brain, and liver corresponding to the predicted DNA product size (Fig. 1A, B) indicating the presence of $\alpha_2\delta_4$ subunit mRNA in these tissues. A second primer pair also yielded a single band at 862 bp (data not shown) corresponding to the predicted size of the $\alpha_2\delta_4$ subunit amplicon (Wycisk et al., 2006a). The

primers used in this study amplify all known isoforms of the $\alpha_2\delta_4$ subunits, and alternatively spliced variants were not detected in our samples, a finding that is in agreement with previous findings (Wycisk et al. 2006a). As a control experiment, water was used in place of template DNA, and no DNA amplification was observed.

The $\alpha_2\delta_4$ subunit protein was present in tissue homogenates from mice and rats using western blotting. A single band with an apparent molecular mass of approximately 170 kDa was detected in homogenates of mouse and rat brain, retina, and liver (Fig. 1C, D). An additional band in the immunoblots of mouse brain had a molecular mass of approximately 165 kDa (Fig. 1D).

Localization of $\alpha_2\delta_4$ subunit in mouse and rat retina

The cellular expression and distribution of the $\alpha_2\delta_4$ subunit was similar in both mouse and rat retina using the same antibody that was used for the western blotting studies. The $\alpha_2\delta_4$ antibody immunostains Muller cells (Fig. 2A,D) and infrequently occurring large cell bodies in the proximal INL (Fig. 2B, E; arrows). These cells, based on their soma size and INL location, are either large amacrine cells or displaced ganglion cells, similar to those previously reported in mouse and rat retinae (Dräger and Olsen, 1980; Abdel-Majid et al., 2005). A diffuse and weak band of immunoreactivity was observed in the OPL of the rat retina (Fig. 2A,B), whereas strongly immunostained puncta were present in the OPL of the mouse retina (Fig. 2D,E). The photoreceptor outer segments and IPL were also weakly immunostained in both species. Immunostaining was absent in sections that were incubated with antibodies preadsorbed with the immunization peptide (Fig. 2C,F), demonstrating the specificity of the antibody. To confirm the presence of the $\alpha_2\delta_4$ subunit in Mu¨ller cells, we performed a double-label immunohistochemistry experiment with an antibody against GS, which labels only Müller cells (Linser et al., 1984). GS and $\alpha_2\delta_4$ subunit immunoreactivities were colocalized in mouse and rat retina (Fig. 3).

Characterization of $\alpha_2\delta_4$ subunit-containing cells in the INL

The cell bodies of bipolar, horizontal, amacrine, and displaced ganglion cells are located in the INL. Based on the cell soma diameter (13 ± 3 μm in mouse and 14 ± 3 lm in rat) and the location of $\alpha_2\delta_4$ subunit immunoreac-tive cells at the border of the INL and IPL, we predicted that these cells were either large amacrine cells or displaced ganglion cells. Amacrine cells are inhibitory neurons, and the majority of these cells utilize glycine or GABA as a neurotransmitter (for review, see Vaney, 1990; Wässle and Boycott, 1991; Kay et al., 2011). Therefore, to evaluate whether $\alpha_2\delta_4$ subunit immunoreactive cells (Fig. 4A,C,E,G; arrowhead) are amacrine cells, we used antibodies to glycine, and to the glutamic acid decarboxylase isoforms, GAD_{65} and GAD_{67}, which catalyze the decarboxylation of glutamate to GABA and CO_2. Antibodies against glycine showed strong immunostaining of amacrine cells in the INL of rat (Fig. 4B) and mouse (Fig. 4F) retina, but immunoreactivity did not colocalize with the $\alpha_2\delta_4$ subunit immunoreactive cells, indicating that these large cells are not glycine-containing amacrine cells. Antibodies against GAD_{65} and GAD_{67} produced immunolabeled somata in the INL and GCL of rat (Fig. 4D) and mouse (Fig. 4H) retina, but again immunoreactivity did not colocalize with the $\alpha_2\delta_4$ subunit immunoreactive cells showing that GABA-containing neurons do not contain $\alpha_2\delta_4$ subunit immunoreactivity. Together these findings indicate that $\alpha_2\delta_4$ subunit immunoreactive cells in the INL are likely to be displaced ganglion cells, and not amacrine cells.

There is no specific marker that is readily available for displaced ganglion cells; therefore, we developed a mouse line with the fluorescent reporter tdTomato localized to subsets of ganglion cells in the GCL and displaced ganglion cells in the INL (Fig. 5B) (Haverkamp et al., 2009; Münch et al., 2009). Some of the $\alpha_2\delta_4$ subunit immunoreactive displaced ganglion

cells express tdTomato, suggesting they contain parvalbumin (Fig. 5C; arrow). In some cases, we were able to visualize the primary dendrites of the labeled cells, which were distributed to the OFF layers of the IPL (Fig. 5C; arrowhead), indicating that these cells are likely to be OFF-type ganglion cells, which have been described previously in the mouse retina (Pang and Wu, 2011).

Characterization of $\alpha_2\delta_4$ subunit puncta localization in the OPL of the mouse retina

The cellular expression of the $\alpha_2\delta_4$ subunit in the OPL was evaluated by using double-labeling immunohistochemistry with specific markers for horizontal, bipolar, and photoreceptor cells in several transgenic mouse lines.

First, we tested whether the $\alpha_2\delta_4$ subunit puncta are located in horizontal cells by using a calbindin antibody, which immunostains all horizontal cells and their processes in the mouse and rat retina (Röhrenbeck et al., 1987; Chun and Wässle, 1993; Massey and Mills, 1996; Haverkamp and Wässle, 2000; Hirano et al., 2005; Gargini et al., 2007). In retinal sections, $\alpha_2\delta_4$ subunit immunoreactive puncta were usually adjacent to horizontal cell endings (Fig. 6A– D). This pattern suggests that these puncta are located either on the adjacent dendritic tips of bipolar cells and/or at the base of the photoreceptors. Retinal sections were also double immunostained with $\alpha_2\delta_4$ subunit and VGAT antibodies. The VGAT antibody immunostains horizontal cell endings in the rodent retina (Cueva et al., 2002; Guo et al., 2010; Lee and Brecha, 2010). The $\alpha_2\delta_4$ subunit immunoreactive puncta did not colocalize with VGAT immunoreactivity. Together, these findings indicate that the $\alpha_2\delta_4$ immunostaining is not localized to horizontal cell somata, processes, or tips (Fig. 6E– H).

To determine whether rod and cone ON-type bipolar cell dendrites express the $\alpha_2\delta_4$ subunit, retinas were immunostained with a Goα antibody to identify ON-type bipolar cells, and a PKC antibody to identify rod bipolar cells (Greferath et al., 1990; Vardi, 1998; Haverkamp and Wässle, 2000). Double labeling of single sections with a z-axis thickness of 0.5 μm showed colocalization of Goα and $\alpha_2\delta_4$ subunit immunoreactivity in the dendrites of ON-type bipolar cells (Fig. 7D; arrowheads). In addition, double labeling of sections showed colocalization of PKC immunoreactivity and $\alpha_2\delta_4$ immunoreactive puncta. $\alpha_2\delta_4$ immunoreactive puncta were located on the distal dendrites of the rod bipolar cells (Fig. 7E–H; arrowheads). In addition to the punctate staining in some rod bipolar cell dendrites, there were numerous $\alpha_2\delta_4$ subunit puncta in the distal OPL that did not colocalize with rod bipolar cell dendrites (Fig. 7H; arrows), suggesting expression of the $\alpha_2\delta_4$ subunit on photoreceptor terminals.

Multiple experiments were performed to test whether photoreceptor terminals express the $\alpha_2\delta_4$ subunit. The first mouse line evaluated was a retinal degeneration (rd1/rd1) mutant, which is characterized by a complete loss of photoreceptors (Carter-Dawson et al., 1978) leading to truncated bipolar cell dendrites (Strettoi and Pignatelli, 2000; Strettoi et al., 2002). Retinal sections of rd1/ rd1 mice stained with PKC and $\alpha_2\delta_4$ subunit antibodies showed a decrease in $\alpha_2\delta_4$ subunit puncta (Fig. 8A) overall compared to the wild-type line. The remaining immunoreactive puncta were colocalized on bipolar cell bodies and their truncated dendritic tips (Fig. 8B–D; arrows). The second line tested was a cone-DTA mutant, which lacks cone photoreceptors 8 months after birth, but rod photoreceptor density and morphology remains normal (Soucy et al., 1998). This mutant was created by expressing the gene for a modified DTA under a promoter selective for cones (Soucy et al., 1998). In these mice (Fig. 8E), $\alpha_2\delta_4$ subunit immunoreactive puncta were usually located distal to the rod bipolar cell tips (Fig. 8H; arrows), indicating their likely presence on rod terminals.

We also examined the location of the $\alpha_2\delta_4$ subunit immunoreactive puncta in cone photoreceptor terminals in wild-type mouse retinae. We began by staining the retina with peanut agglutinin (PNA), which is a specific marker for cone pedicle bases in mouse retina (Blanks and Johnson, 1983). Single scans revealed that the $\alpha_2\delta_4$ subunit immunoreactive puncta were often near the base of the PNA-stained cone pedicles (Fig. 8I – K).

To further test whether $\alpha_2\delta_4$ subunit immunoreactive puncta are expressed by rod and cone photoreceptor terminals, we evaluated $\alpha_2\delta_4$ immunostaining relative to the photoreceptor synaptic ribbon by using antibodies to bassoon and CtBP2. The presynaptic protein bassoon is associated with the base of the synaptic ribbon in rod spherules and cone pedicles (Brandstätter et al., 1999), and CtBP2 is localized to the ribbon proper (Brandstätter et al., 1999; Schmitz et al., 2000). The immunostaining of bassoon and CtBP2 together form a shallow arc, with bassoon immunoreactivity surrounded by CtBP2 immunoreactivity (tom Dieck et al., 2005). The $\alpha_2\delta_4$ subunit immunoreactive puncta do not overlap with the CtBP2-immunolabeled ribbons, and they often appear to be adjacent to CtBP2-immunostained puncta (Fig. 9D; arrows). In contrast, bassoon immunostaining showed slight overlap with some $\alpha_2\delta_4$ subunit puncta (Fig. 9E–H; arrows), indicating that $\alpha_2\delta_4$ subunits are located at or close to the base of the synaptic ribbon (tom Dieck et al., 2005). We also double immunostained the retinas with an antibody against PSD-95, which is located in the plasma membrane of rod and cone photoreceptor terminals (Koulen et al., 1998). Figure 9I – L shows a single scan of a section through the OPL double labeled for PSD-95 and the $\alpha_2\delta_4$ subunit. Most PSD-95-immunolabeled photoreceptor terminals contained $\alpha_2\delta_4$ immunoreactive puncta (Fig. 9L; arrows).

Together, these findings indicate that $\alpha_2\delta_4$ subunit immunoreactivity is mainly associated with rod spherules and ON-type bipolar cell dendrites in the OPL. We could not establish whether $\alpha_2\delta_4$ subunit puncta were located at cone pedicles (see Discussion), although this could not be ruled out.

DISCUSSION

The accessory Ca channel subunit $\alpha_2\delta_4$ is localized to Mu¨ller cells, ON-type bipolar cells, displaced ganglion cells, and photoreceptors. We did not observe $\alpha_2\delta_4$ subunit immunoreactivity in amacrine or ganglion cell bodies that were located in the INL or GCL, respectively. However, there was some weak immunostaining in the IPL, suggesting that the $\alpha_2\delta_4$ subunit could also be located at processes in this layer.

$\alpha_2\delta_4$ subunit expression

The $\alpha_2\delta_4$ subunit is expressed in non-neuronal endocrine cells (Arikkath and Campbell, 2003; Canti et al., 2003; Klugbauer et al., 2003) and recently, $\alpha_2\delta_4$ subunit immunoreactivity was localized to salamander photoreceptor terminals (Mercer et al., 2011). The present findings extend this earlier observation in the retina, and show that this subunit is also expressed in Mu¨ller cells, some bipolar cell dendrites, and a few displaced ganglion cells in the mouse and rat retina. $\alpha_2\delta_4$ mRNA was also detected in brain and liver (Fig. 1A,B) consistent with earlier findings (Wycisk et al., 2006a).

$\alpha_2\delta$ subunit isoforms have been identified in a variety of cell lines and tissues (Ellis et al., 1988; Kim et al., 1992; Brust et al., 1993; Gilad et al., 1995). Alternatively spliced $\alpha_2\delta_4$ subunits have been reported in kidney, muscle, spleen, and stomach, but not in the brain or retina (this study; Wycisk et al., 2006a). However, in our western blots of mouse brain there is an additional band with a molecular weight of ~165 kDa (Fig. 1D). This band, which is shifted from the major ~170 kDa band, could be a degradation product, or an uncharacterized $\alpha_2\delta_4$ subunit isoform.

Functional role of $\alpha_2\delta$ subunits

Mouse mutants and knockout mice lacking functional $\alpha_2\delta$ subunits have a spectrum of abnormal physiological properties, including cardiovascular dysfunction, neuro-degeneration, neuropathic pain, and epilepsy (Snell, 1955; Fuller-Bicer et al., 2009; Neely et al., 2010). For example, the Cacna2d1 knockout mouse line is characterized by alterations of the biophysical properties of L-type Ca^{2+} currents in cardiomyocytes (Fuller-Bicer et al., 2009). The Cacna2d2 mutant mouse line, known as "ducky," has been used as an animal model for absence epilepsy, and this line is characterized by spike-wave seizures, cerebellar degeneration, and ataxia (Snell, 1955). The Cacna2d3 knockout mouse line does not show any gross anatomical changes of the brain; however, mice with the $\alpha_2\delta_3$ subunit deletion exhibit impaired sensitivity to thermal pain (Neely et al., 2010).

Mice with a frameshift mutation producing an early truncation of the Cacna2d4 transcript have an altered ERG and a loss of ribbon synapses in rod photoreceptors, as well as poorly developed ribbon synapses in cone photoreceptors (Ruether et al., 2000; Wycisk et al., 2006a,b). These findings suggest an essential role of the $\alpha_2\delta_4$ subunit in outer retinal structure and function, although it is unclear whether deletion of the $\alpha_2\delta_4$ subunit directly or indirectly causes these functional and structural abnormalities. The $\alpha_2\delta$ subunits are a component of voltage-activated Ca channels, and these subunits modify Ca channel function by influencing channel trafficking, namely, the intracellular transport of the α_1 protein to increase the functional expression of Ca channels (Dolphin, 2012). In addition, $\alpha_2\delta$ subunits can also alter the biophysical properties of Ca channels (Catterall et al., 1993; Snutch et al., 2005; Dolphin, 2012). Cacna2d1 knockout mice show reduced cardiac L-type Ca^{2+} currents (Fuller-Bicer et al., 2009), and Cacna2d2 knockout mice have reduced cerebellar Purkinje cell P/Q-type Ca^{2+} currents (Barclay et al., 2001; Brodbeck et al., 2002). On this basis, deletions of the $\alpha_2\delta_4$ subunit could lead to an alteration of neuronal and Müller cell Ca^{2+} currents. The reduction of the b-wave in Cacna2d4 mice (Wycisk et al., 2006a) could be due to a disruption of the Ca channel mediating neurotransmission from photoreceptors to bipolar cells. This idea is supported by studies showing the reduction or elimination of the b-wave in mouse lines with mutations in the α_{1F} subunit (Chang et al., 2006; Lodha et al., 2010) or the β2 accessory sub-unit (Ball et al., 2002), which are expressed in photoreceptors.

$\alpha_2\delta_4$ subunit expression in the outer retina

The $\alpha_2\delta_4$ subunit is expressed in rod photoreceptor spherules based on its colocalization with PSD-95, which is located presynaptically in photoreceptor terminals (Koulen et al., 1998). These findings are also consistent with the reported localization of the $\alpha_2\delta_4$ subunit to salamander photoreceptor terminals (Mercer et al., 2011). As mentioned above, the localization of the $\alpha_2\delta_4$ subunit to photoreceptor terminals is also consistent with the altered ERG and cellular abnormalities seen in the Cac-na2d4 mutants (Wycisk et al., 2006a,b). Alterations of the $\alpha_2\delta_4$ subunit in photoreceptor terminals could lead to altered trafficking of the α_1 subunit, resulting in dysfunctional activity of the channel and the cellular abnormalities observed by Wycisk et al (2006a). We could not demonstrate the presence of the $\alpha_2\delta_4$ subunit in cone photoreceptor terminals. However, some $\alpha_2\delta_4$ subunit puncta were adjacent to the PNA labeling, suggesting the possibility that the $\alpha_2\delta_4$ subunit is also expressed in cone pedicles (Fig. 8C).

$\alpha_2\delta_4$ subunit expression in the inner retina

The $\alpha_2\delta_4$ subunit is expressed by OFF-type displaced ganglion cells and it is unlikely to be expressed by large amacrine cells based on two findings: 1) large cells that are $\alpha_2\delta_4$ subunit immunoreactive do not contain glycine or GAD immunoreactivity, which are typically expressed by amacrine cells (Fig. 4); and 2) some of the tdTomatofluorescent displaced

ganglion cells in the PV-cre × ROSA26-tdTomato line express the $\alpha_2\delta_4$ subunit (Fig. 5). Furthermore, not all tdTomato-positive, displaced ganglion cells express the $\alpha_2\delta_4$ subunit (not shown). This differential expression suggests some molecular differences in displaced ganglion cells.

$\alpha_2\delta_4$ subunit expression in Müller cells

Müller cells, which are retinal glia cells, express multiple voltage-activated channels and they regulate extracellular K^+ and H^+, as well as take up extracellular glutamate and GABA (Newman and Reichenbach, 1996). Müller cells also express the $\alpha_2\delta_4$ subunit, and this subunit is likely to be associated with L-type subunits that are expressed by Müller cells (Puro et al., 1996; Nachman-Clewner et al., 1999; Xu et al., 2002; Welch et al., 2005). Interestingly, in the Cacna2d4 mutant there is no disruption of the c-wave of the ERG (Ruether et al., 2000). The c-wave of the ERG, which is attributed to Müller cells and retinal pigmented epithelial cells, may not be sensitive to changes in Müller cell Ca^{2+} signaling or perhaps there is a compensation by other voltage-gated Ca channel subunits.

The α_{1F} subunit (Cav1.4) is likely to be associated with the $\alpha_2\delta_4$ subunit based on its presence on salamander photoreceptor terminals (Mercer et al., 2011). This could also be the case for the rodent retina, because the $\alpha_2\delta_4$ subunit is expressed on photoreceptor terminals, and the Cacna1F knockout mouse lacks synaptic signaling in the outer retina and shows degeneration of their photoreceptor ribbon terminals (Mansergh et al., 2005; Chang et al., 2006). Other a_1 subunit candidates that may associate with the $\alpha_2\delta_4$ subunit are the α_{1C} and α_{1D} subunits, which are involved in neurotransmission and synaptic plasticity at photoreceptor synapses (Puro et al., 1996; Nachman-Clewner et al., 1999; Xu et al., 2002; Mize at al., 2002), and are in Müller cells of rat and salamander retinas (Puro et al., 1996; Nachman-Clewner et al., 1999; Xu et al., 2002; Welch et al., 2005).

Previous studies (Eroglu et al., 2009; Kurshan et al., 2009) have shown that $\alpha_2\delta$ subunits are also involved in synaptogenesis, independent of their association with Ca channels, and suggest that these subunits are important for synaptic stabilization. Deficits of synaptic stabilization could also explain photoreceptor-bipolar cell synapse disruption in mice with a mutation in the $\alpha_2\delta_4$ subunit. This is the case for the $\alpha_2\delta_4$ subunit, which is required for thrombospondin- and astrocyte-induced synapse formation in rodents (Eroglu et al., 2009), and the $\alpha_2\delta_3$ subunit, which is required for the stabilization of the α_1 subunit and synaptogenesis in *Drosophila* (Dickman et al., 2008; Ly et al., 2008; Kurshan et al., 2009). Furthermore, $\alpha_2\delta$ subunits may not be present at the Ca channel under normal conditions (Davies et al., 2007) and they may only be present when the α_1 subunits are inserted into the plasma membrane or trafficked from intracellular compartments. We therefore cannot rule out additional functional roles for the $\alpha_2\delta_4$ subunit in the retina. Finally, Ca channels have not been reported in photoreceptor outer segments (Rispoli et al., 1991; Križaj, 2012), suggesting that $\alpha_2\delta_4$ subunits have a functional role in this structure that is not associated with Ca^{2+} currents. One possible explanation is that $\alpha_2\delta_4$ subunits participate in trafficking membrane proteins to the outer segments.

In conclusion, the $\alpha_2\delta_4$ subunit is likely to have a critical regulatory role in the outer retina, and influence both photoreceptor terminal structure and neurotransmission in the synaptic triad and at basal contacts. However, to better understand the functional role of $\alpha_2\delta_4$ subunits in the retina, further studies are required, including electron microscopy to determine its exact location and distribution at presynaptic and postsynaptic sites. In addition, electrophysiological recordings of photoreceptor, bipolar, and Müller cells, as well as ERG measurements would be of value for determining whether the $\alpha_2\delta_4$ subunit is associated with α_1 subunits, and whether there is any compensation by other Ca channel subunits in the Cacna2d4 knockout mouse line.

Acknowledgments

We thank Drs. Steven Barnes and Arlene Hirano for their comments and discussion on this project and manuscript. We thank Dr. Deborah Farber for the rd1 mice, and Drs. Michael Gorin and Anna Matynia for the cone-DTA mice.

Grant sponsor: the U.S. Army Medical Research & Materiel Command (USAMRMC) and the Telemedicine & Advanced Technology Research Center (TATRC), at Fort Detrick, MD; Grant number: W81XWH-10-2-0077; Grant sponsor: National Institutes of Health; Grant number: EY04067; Grant sponsor: Veterans Administration Merit Review (to N.C.B., who is also a Veterans Administration Career Research Scientist) J.L. and A.S. contributed equally to this work.

ROLE OF AUTHORS

All authors had full access to all the data in the study and take responsibility for the integrity of the data and the accuracy of the data analysis. Study concept and design: L.P.S and N.B. Acquisition of data: L.P.S., J.L., A.S., and A.R. Analysis and interpretation of data: L.P.S., J.L., A.S., A.R., and N.B. Drafting of the manuscript: L.P.S and N.B. Critical revision of the manuscript for important intellectual content: L.P.S and N.B. Obtained funding: N.B. Administrative, technical, and material support: A.S. and A.R. Study supervision: L.P.S and N.B.

LITERATURE CITED

Abdel-Majid RM, Archibald ML, Tremblay F, Baldridge WH. Tracer coupling of neurons in the rat retina inner nuclear layer labeled by Fluorogold. Brain Res. 2005; 1063:114–120. [PubMed: 16263096]

Angelotti T, Hofmann F. Tissue-specific expression of splice variants of the mouse voltage-gated calcium channel alpha2/delta subunit. FEBS Lett. 1996; 397:331–337. [PubMed: 8955374]

Arikkath J, Campbell KP. Auxiliary subunits: essential components of the voltage-gated calcium channel complex. Curr Opin Neurobiol. 2003; 13:298–307. [PubMed: 12850214]

Ball SL, Powers PA, Shin HS, Morgans CW, Peachey NS, Gregg RG. Role of the beta(2) subunit of voltage-dependent calcium channels in the retinal outer plexiform layer. Invest Ophthalmol Vis Sci. 2002; 43:1595–1603. [PubMed: 11980879]

Barclay J, Balaguero N, Mione M, Ackerman SL, Letts VA, Brodbeck J, Canti C, Meir A, Page KM, Kusumi K, Perez-Reyes E, Lander ES, Frankel WN, Gardiner RM, Dolphin AC, Rees M. Ducky mouse phenotype of epilepsy and ataxia is associated with mutations in the Cacna2d2 gene and decreased calcium channel current in cerebellar Purkinje cells. J Neurosci. 2001; 21:6095–6104. [PubMed: 11487633]

Bauer CS, Tran-Van-Minh A, Kadurin I, Dolphin AC. A new look at calcium channel $\alpha_2\delta$ subunits. Curr Opin Neurobiol. 2010; 20:563–571. [PubMed: 20579869]

Blanks JC, Johnson LV. Selective lectin binding of the developing mouse retina. J Comp Neurol. 1983; 221:31–41. [PubMed: 6643744]

Brandstätter JH, Fletcher EL, Garner CC, Gundelfinger ED, Wässle H. Differential expression of the cytomatrix protein bassoon among ribbon synapses in the mammalian retina. Eur J Neurosci. 1999; 11:3683–3693. [PubMed: 10564375]

Brecha NC, Sternini C, Humphrey MF. Cellular distribution of L-glutamate decarboxylase (GAD) and gamma-aminobutyric acidA (GABAA) receptor mRNAs in the retina. Cell Mol Neurobiol. 1991; 11:497–509. [PubMed: 1660350]

Brodbeck J, Davies A, Courtney JM, Meir A, Balaguero N, Canti C, Moss FJ, Page KM, Pratt WS, Hunt SP, Barclay J, Rees M, Dolphin AC. The ducky mutation in Cacna2d2 results in altered Purkinje cell morphology and is associated with the expression of a truncated alpha 2 delta-2 protein with abnormal function. J Biol Chem. 2002; 277:7684–7693. [PubMed: 11756448]

Brust PF, Simerson S, McCue AF, Deal CR, Schoonmaker S, Williams ME, Velicelebi G, Johnson EC, Harpold MM, Ellis SB. Human neuronal voltage-dependent calcium channels: studies on subunit structure and role in channel assembly. Neuropharmacology. 1993; 32:1089–1102. [PubMed: 8107964]

Canti C, Davies A, Dolphin AC. Calcium channel a_2d subunits: structure, functions and target site for drugs. Curr Neuropharmacol. 2003; 1:209–217.

Carter-Dawson LD, LaVail MM, Sidman RL. Differential effect of the rd mutation on rods and cones in the mouse retina. Invest Ophthalmol Vis Sci. 1978; 17:489–498. [PubMed: 659071]

Caterall WA. Structure and regulation of voltage-gated Ca2+ channels. Annu Rev Cell Dev Biol. 2000; 16:521–555. [PubMed: 11031246]

Catterall WA, de Jongh K, Rotman E, Hell J, Westenbroek R, Dubel SJ, Snutch TP. Molecular properties of calcium channels in skeletal muscle and neurons. Ann N Y Acad Sci. 1993; 681:342–355. [PubMed: 8395149]

Chang B, Heckenlively JR, Bayley PR, Brecha NC, Davisson MT, Hawes NL, Hirano AA, Hurd RE, Ikeda A, Johnson BA, McCall MA, Morgans CW, Nusinowitz S, Peachey NS, Rice DS, Vessey KA, Gregg RG. The nob2 mouse, a null mutation in Cacna1f: anatomical and functional abnormalities in the outer retina and their consequences on ganglion cell visual responses. Vis Neurosci. 2006; 23:11–24. [PubMed: 16597347]

Chang YC, Gottlieb DI. Characterization of the proteins purified with monoclonal antibodies to glutamic acid decar-boxylase. J Neurosci. 1988; 8:2123–2130. [PubMed: 3385490]

Chun MH, Wässle H. Some horizontal cells of the bovine retina receive input synapses in the inner plexiform layer. Cell Tissue Res. 1993; 272:447–457. [PubMed: 8339319]

Cole RL, Lechner SM, Williams ME, Prodanovich P, Bleicher L, Varney MA, Gu G. Differential distribution of voltage-gated calcium channel α_2-δ ($\alpha_2\delta$) subunit mRNA-containing cell in the rat central nervous system and the dorsal root ganglia. J Comp Neurol. 2005; 491:246–269. [PubMed: 16134135]

Cueva JG, Haverkamp S, Reimer RJ, Edwards R, Wässle H, Brecha NC. Vesicular gamma-aminobutyric acid transporter expression in amacrine and horizontal cells. J Comp Neurol. 2002; 445:227–237. [PubMed: 11920703]

Davies A, Hendrich J, Van Minh AT, Wratten J, Douglas L, Dolphin AC. Functional biology of the alpha(2)delta subunits of voltage-gated calcium channels. Trends Pharmacol Sci. 2007; 28:220–228. [PubMed: 17403543]

Dhingra A, Lyubarsky A, Jiang M, Pugh EN Jr, Birnbaumer L, Sterling P, Vardi N. The light response of ON bipolar neurons requires $G\alpha_o$. J Neurosci. 2000; 20:9053–9058. [PubMed: 11124982]

Dick O, tom Dieck S, Altrock WD, Ammermüller J, Weiler R, Garner CC, Gundelfinger ED, Brandstätter JH. The presynaptic active zone protein bassoon is essential for photoreceptor ribbon synapse formation in the retina. Neuron. 2003; 37:775–786. [PubMed: 12628168]

Dickman DK, Kurshan PT, Schwarz TL. Mutations in a Drosophila alpha2delta voltage-gated calcium channel subunit reveal a crucial synaptic function. J Neurosci. 2008; 28:31–38. [PubMed: 18171920]

Dolphin AC. Calcium channel auxiliary α2δ and β subunits: trafficking and one step beyond. Nat Rev Neurosci. 2012; 13:542–555. [PubMed: 22805911]

Dräger UC, Olsen JF. Origins of crossed and uncrossed retinal projections in pigmented and albino mice. J Comp Neurol. 1980; 191:383–412. [PubMed: 7410600]

Ellis SB, Williams ME, Ways NR, Brenner R, Sharp AH, Leung AT, Campbell KP, McKenna E, Koch WJ, Hui A, Schartz A, Haroold MM. Sequence and expression of mRNAs encoding the alpha 1 and alpha 2 subunits of a DHP-sensitive calcium channel. Science. 1988; 241:1661–1664. [PubMed: 2458626]

Erlander MG, Tillakaratne NJ, Feldblum S, Patel N, Tobin AJ. Two genes encode distinct glutamate decarboxylases. Neuron. 1991; 7:91–100. [PubMed: 2069816]

Eroglu C, Allen NJ, Susman MW, O'Rourke NA, Park CY, Ozkan E, Chakraborty C, Mulinyawe SB, Annis DS, Huberman AD, Green EM, Lawler J, Dolmetsch R, Garcia KC, Smith SJ, Luo ZD, Rosenthal A, Mosher DF, Barres BA. Gabapentin receptor alpha2delta-1 is a neuronal thrombospondin receptor responsible for excitatory CNS synaptogenesis. Cell. 2009; 139:380–392. [PubMed: 19818485]

Fong AY, Stornetta RL, Foley CM, Potts JT. Immunohistochemical localization of GAD67-expressing neurons and processes in the rat brainstem: subregional distribution in the nucleus tractus solitarius. J Comp Neurol. 2005; 493:274–290. [PubMed: 16255028]

Fuller-Bicer GA, Varadi G, Koch SE, Ishii M, Bodi I, Kadeer N, Muth JN, Mikala G, Petrashevskaya NN, Jordan MA, Zhang SP, Qin N, Flores CM, Isaacsohn I, Varadi M, Mori Y, Jones WK,

Schwartz A. Targeted disruption of the voltage-dependent calcium channel alpha2/delta-1-subunit. Am J Physiol Heart Circ Physiol. 2009; 297:H117–H124. [PubMed: 19429829]

Gao B, Sekido Y, Maximov A, Saad M, Forgacs E, Latif F, Wei MH, Lerman M, Lee JH, Perez-Reyes E, Bezprozvanny I, Minna JD. Functional properties of a new voltage-dependent calcium channel a2d auxiliary subunit gene (CAC-NA2D2). J Biol Chem. 2000; 275:12237–12242. [PubMed: 10766861]

Gargini C, Terzibasi E, Mazzoni F, Strettoi E. Retinal organization in the retinal degeneration 10 (rd10) mutant mouse: a morphological and ERG study. J Comp Neurol. 2007; 500:222–238. [PubMed: 17111372]

Ghosh KK, Haverkamp S, Wässle H. Glutamate receptors in the rod pathway of the mammalian retina. J Neurosci. 2001; 21:8636–8647. [PubMed: 11606651]

Gilad B, Shenkar N, Halevi S, Trus M, Atlas D. Identification of the alternative spliced form of the alpha 2/delta subunit of voltage sensitive Ca2+ channels expressed in PC12 cells. Neurosci Lett. 1995; 193:157–160. [PubMed: 7478172]

Gong HC, Hang J, Kohler W, Li L, Su TZ. Tissue-specific expression and gabapentin-binding proteins properties of calcium channel subunit alpha2delta subunit subtypes. J Membr Biol. 2001; 184:35–43. [PubMed: 11687876]

Greferath U, Grünert U, Wässle H. Rod bipolar cells in the mammalian retina show protein kinase C-like immuno-reactivity. J Comp Neurol. 1990; 301:433–442. [PubMed: 2262600]

Guo C, Stella SL, Hirano AA, Brecha N. Plasmalemmal and vesicular-aminobutyric acid transporter expression in the developing mouse retina. J Comp Neurol. 2009; 512:6–26. [PubMed: 18975268]

Guo C, Hirano AA, Stella SL, Bitzer M, Brecha NC. Guinea pig horizontal cells express GABA, the GABA-synthesizing enzyme GAD65, and the GABA vesicular transporter. J Comp Neurol. 2010; 518:1647–1669. [PubMed: 20235161]

Hagino-Yamagishi K, Nakazawa H. Involvement of Ga(olf)-expressing neurons in the vomeronasal system of *Bufo japonicus* . J Comp Neurol. 2011; 519:3189–3201. [PubMed: 21618228]

Haverkamp S, Wässle H. Immunocytochemical analysis of the mouse retina. J Comp Neurol. 2000; 424:1–23. [PubMed: 10888735]

Haverkamp S, Ghosh KK, Hirano AA, Wässle H. Immunocytochemical description of five bipolar cell types of the mouse retina. J Comp Neurol. 2003; 455:463–476. [PubMed: 12508320]

Haverkamp S, Inta D, Monyer H, Wässle H. Expression analysis of green fluorescent protein in retinal neurons of four transgenic mouse lines. Neuroscience. 2009; 160:126–139. [PubMed: 19232378]

Heusner CL, Beutler LR, Houser CR, Palmiter RD. Deletion of GAD67 in dopamine receptor-1 expressing cells causes specific motor deficits. Genesis. 2008; 46:357–367. [PubMed: 18615733]

Hirano AA, Brandstätter JH, Brecha NC. Cellular distribution and subcellular localization of molecular components of vesicular transmitter release in horizontal cells of rabbit retina. J Comp Neurol. 2005; 488:70–81. [PubMed: 15912504]

Jusuf PR, Martin PR, Grünert U. Synaptic connectivity in the midget-parvocellular pathway of primate central retina. J Comp Neurol. 2006; 494:260–274. [PubMed: 16320234]

Kay JN, Voinescu PE, Chu MW, Sanes JR. Neurod6 expression defines new retinal amacrine cell subtypes and regulates their fate. Nat Neurosci. 2011; 14:965–972. [PubMed: 21743471]

Kim HL, Kim H, Lee P, King RG, Chin H. Rat brain expresses an alternatively spliced form of the dihydropyridine-sensitive L-type calcium channel alpha 2 subunit. Proc Natl Acad Sci U S A. 1992; 89:3251–3255. [PubMed: 1314383]

Klugbauer N, Lacinová L, Marais E, Hobom M, Hofmann F. Molecular diversity of the calcium channel $\alpha_2\delta$ subunit. J Neurosci. 1999; 19:684–691. [PubMed: 9880589]

Klugbauer N, Marais E, Hofmann F. Calcium channel alpha2delta subunits: differential expression, function, and drug binding. J Bioenerg Biomembr. 2003; 35:671–685. [PubMed: 15000527]

Koulen P, Fletcher EL, Craven SE, Bredt DS, Wässle H. Immunocytochemical localization of the postsynaptic density protein PSD-95 in the mammalian retina. J Neurosci. 1998; 18:10136–10149. [PubMed: 9822767]

Križaj D. Calcium stores in vertebrate photoreceptors. Adv Exp Med Biol. 2012; 740:873–889. [PubMed: 22453974]

Kurshan PT, Oztan A, Schwarz TL. Presynaptic alpha(2)-delta-3 is required for synaptic morphogenesis independent of its Ca(2+)-channel functions. Nat Neurosci. 2009; 12:1415–1423. [PubMed: 19820706]

Lee H, Brecha NC. Immunocytochemical evidence for SNARE protein-dependent transmitter release from guinea pig horizontal cells. Eur J Neurosci. 2010; 31:1388–1401. [PubMed: 20384779]

Linser PJ, Sorrentino M, Moscona AA. Cellular compartmentalization of carbonic anhydrase-C and glutamine synthetase in developing and mature mouse neural retina. Brain Res. 1984; 315:65–71. [PubMed: 6144368]

Lodha N, Bonfield S, Orton NC, Doering CJ, McRory JE, Mema SC, Rehak R, Sauve Y, Tobias R, Stell WK, Bech-Hansen NT. Congenital stationary night blindness in mice—a tale of two Cacna1f mutants. Adv Exp Med Biol. 2010; 664:549–558. [PubMed: 20238058]

Ly CV, Yao CK, Verstreken P, Ohyama T, Bellen HJ. Straightjacket is required for the synaptic stabilization of cacophony, a voltage-gated calcium channel alpha1 subunit. J Cell Biol. 2008; 181:157–170. [PubMed: 18391075]

Mansergh F, Orton NC, Vessey JP, Lalonde MR, Stell WK, Tremblay F, Barnes S, Rancourt DE, Bech-Hansen NT. Mutation of the calcium channel gene Cacna1f disrupts calcium signaling, synaptic transmission and cellular organization in mouse retina. Hum Mol Genet. 2005; 14:3035–3046. [PubMed: 16155113]

Massey SC, Mills SL. A calbindin-immunoreactive cone bipolar cell type in the rabbit retina. J Comp Neurol. 1996; 366:15–33. [PubMed: 8866843]

McIntire SL, Reimer RJ, Schuske K, Edwards RH, Jorgensen EM. Identification and characterization of the vesicular GABA transporter. Nature. 1997; 389:870–876. [PubMed: 9349821]

Mercer AJ, Chen M, Thoreson WB. Lateral mobility of presynaptic L-type calcium channels at photoreceptor ribbon synapses. J Neurosci. 2011; 31:4397–4406. [PubMed: 21430141]

Mize RR, Graham SK, Cork RJ. Expression of the L-type calcium channel in the developing mouse visual system by use of immunocytochemistry. Brain Res Dev Brain Res. 2002; 136:185–195.

Münch TA, da Silveira RA, Siegert S, Viney TJ, Awatramani GB, Roska B. Approach sensitivity in the retina processed by a multifunctional neural circuit. Nat Neurosci. 2009; 12:1308–1316. [PubMed: 19734895]

Nachman-Clewner M, St Jules R, Townes-Anderson E. L-type calcium channels in the photoreceptor ribbon synapse: localization and role in plasticity. J Comp Neurol. 1999; 415:1–16. [PubMed: 10540354]

Neely GG, Hess A, Costigan M, Keene AC, Goulas S, Langeslag M, Griffin RS, Belfer I, Dai F, Smith SB, Diatchenko L, Gupta V, Xia CP, Amann S, Kreitz S, Heindl-Erdmann C, Wolz S, Ly CV, Arora S, Sarangi R, Dan D, Novatchkova M, Rosenzweig M, Gibson DG, Truong D, Schramek D, Zoranovic T, Cronin SJ, Angjeli B, Brune K, Dietzl G, Maixner W, Meixner A, Thomas W, Pospisilik JA, Alenius M, Kress M, Subramaniam S, Garrity PA, Bellen HJ, Woolf CJ, Penninger JM. A genome-wide Drosophila screen for heat nociception identifies α2δ3 as an evolutionary conserved pain gene. Cell. 2010; 143:628–638. [PubMed: 21074052]

Newman E, Reichenbach A. The Müller cell: a functional element of the retina. TINS. 1996; 19:307–312. [PubMed: 8843598]

Pang JJ, Wu SM. Morphology and immunoreactivity of retrogradely double-labeled ganglion cells in the mouse retina. Invest Ophthalmol Vis Sci. 2011; 52:4886–4896. [PubMed: 21482641]

Pow DV, Hendrickson AE. Distribution of the glycine transporter glyt-1 in mammalian and nonmammalian retinae. Vis Neurosci. 1999; 16:231–239. [PubMed: 10367958]

Pow DV, Wright LL, Vaney DI. The immunocytochemical detection of amino-acid neurotransmitters in paraformalde-hyde-fixed tissues. J Neurosci Methods. 1995; 56:115–123. [PubMed: 7752677]

Puller C, Haverkamp S, Grünert U. OFF midget bipolar cells in the retina of the marmoset, *Callithrix jacchus*, express AMPA receptors. J Comp Neurol. 2007; 502:442–454. [PubMed: 17366611]

Puro DG, Hwang JJ, Kwon OJ, Chin H. Characterization of an L-type calcium channel expressed by human retinal Muller (glial) cells. Mol Brain Res. 1996; 37:41–48. [PubMed: 8738134]

Qin N, Yagel S, Momplaisir ML, Codd EE, D'Andrea MR. Molecular cloning and characterization of the human voltage-gated calcium channel alpha(2)delta-4 subunit. Mol Pharmacol. 2002; 62:485–496. [PubMed: 12181424]

Rispoli G, Sather WA, Detwiler PB. Visual transduction in dialysed detached rod outer segments from lizard retina. J Physiol. 1993; 465:513–537. [PubMed: 8229848]

Röhrenbeck J, Wässle H, Heizmann CW. Immunocytochemical labelling of horizontal cells in mammalian retina using antibodies against calcium-binding proteins. Neurosci Lett. 1987; 77:255–260. [PubMed: 3302765]

Ruether K, Grosse J, Matthiessen E, Hoffman K, Hartmann C. Abnormalities of the photoreceptor-bipolar cell synapse in a substrain of C57BL/10 mice. Invest Opththalmol Vis Sci. 2000; 41:4039–4047.

Sagné C, El Mestikawy S, Isambert MF, Hamon M, Henry JP, Giros B, Gasnier B. Cloning of a functional vesicular GABA and glycine transporter by screening of genome databases. FEBS Lett. 1997; 417:177–183. [PubMed: 9395291]

Schlick B, Flucher BE, Obermair GJ. Voltage-activated calcium channel expression profiles in mouse brain and cultured hippocampal neurons. Neuroscience. 2010; 167:786–798. [PubMed: 20188150]

Schmitz F, Königstorfer A, Südhof TC. RIBEYE, a component of synaptic ribbons: a protein's journey through evolution provides insight into synaptic ribbon function. Neuron. 2000; 28:857–872. [PubMed: 11163272]

Snell GD. Ducky, a new second chromosome mutation in the mouse. J Hered. 1955; 46:27–29.

Snutch, TP.; Peloquin, J.; Mathews, E.; McRoy, JE. Molecular properties of voltage-gated calcium channels. In: Zamponi, GW., editor. Voltage-gated calcium channels. New York: Springer, Landes Biosciences; 2005. p. 61-94.

Soucy E, Wang Y, Nirenberg S, Nathans J, Meister M. A novel signaling pathway from rod photoreceptors to ganglion cells in mammalian retina. Neuron. 1998; 21:481–493. [PubMed: 9768836]

Strettoi E, Pignatelli V. Modifications of retinal neurons in a mouse model of retinitis pigmentosa. Proc Natl Acad Sci U S A. 2000; 97:11020–11025. [PubMed: 10995468]

Strettoi E, Porciatti V, Falsini B, Pignatelli V, Rossi C. Morphological and functional abnormalities in the inner retina of the rd/rd mouse. J Neurosci. 2002; 22:5492–5504. [PubMed: 12097501]

Tom Dieck S, Sanmarti-Vila L, Langnaese K, Richter K, Kindler S, Soyke A, Wex H, Smalla KH, Kampf U, Franzer JT, Stumm M, Garner CC, Gundelfinger ED. Bassoon, a novel zinc-finger AG/glutaminerepeat protein selectively localized at the active zone of presynaptic nerve terminals. J Cell Biol. 1998; 142:499–509. [PubMed: 9679147]

tom Dieck S, Altrock WD, Kessels MM, Qualmann B, Regus H, Brauner D, Fejtova A, Bracko O, Gundelfinger ED, Brandstätter JH. Molecular dissection of the photoreceptor ribbon synapse: physical interaction of bassoon and RIBEYE is essential for the assembly of the ribbon complex. J Cell Biol. 2005; 168:825–836. [PubMed: 15728193]

Vaney DI. The mosaic of amacrine cells in the mammalian retina. Prog Ret Res. 1990; 9:49–100.

Vardi N. Alpha subunit of Go localizes in the dendritic tips of ON bipolar cells. J Comp Neurol. 1998; 395:43–52. [PubMed: 9590545]

Wässle H, Boycott BB. Functional architecture of the mammalian retina. Physiol Rev. 1991; 71:447–480. [PubMed: 2006220]

Welch NC, Wood S, Jollimore C, Stevens K, Kelly ME, Barnes S. High-voltage-activated calcium channels in Muller cells acutely isolated from tiger salamander retina. Glia. 2005; 49:259–274. [PubMed: 15472989]

Wycisk KA, Budde B, Feil S, Skosyrski S, Buzzi F, Neidhardt J, Glaus E, Nürnberg P, Ruether K, Berger W. Structural and functional abnormalities of retinal ribbon synapses due to Cacna2d4 mutation. Invest Ophthalmol Vis Sci. 2006a; 47:3523–3530. [PubMed: 16877424]

Wycisk KA, Zeitz C, Feil S, Wittmer M, Forster U, Neidhardt J, Wissinger B, Zrenner E, Wilke R, Kohl S, Berger W. Mutation in the auxiliary calcium-channel subunit Cacna2d4 causes autosomal recessive cone dystrophy. Am J Hum Genet. 2006b; 79:973–977. [PubMed: 17033974]

Xu HP, Zhao JW, Yang XL. Expression of voltage-dependent calcium channel subunits in the rat retina. Neuro-sci Lett. 2002; 329:297–300.

Yamamoto T, Yamato E, Tashiro F, Sato T, Noso S, Ikegami H, Tamura S, Yanagawa Y, Miyazaki JI. Development of autoimmune diabetes in glutamic acid decarboxylase 65 (GAD65) knockout NOD mice. Diabetologia. 2004; 47:221–224. [PubMed: 14676944]

Young S, Rothbard J, Parker PJ. A monoclonal antibody recognizing the site of limited proteolysis of protein kinase C. Eur J Biochem. 1988; 173:247–252. [PubMed: 2451608]

Zhang J, Yang Z, Wu SM. Development of cholinergic amacrine cells is visual activity-dependent in the postnatal mouse retina. J Comp Neurol. 2005; 484:331–343. [PubMed: 15739235]

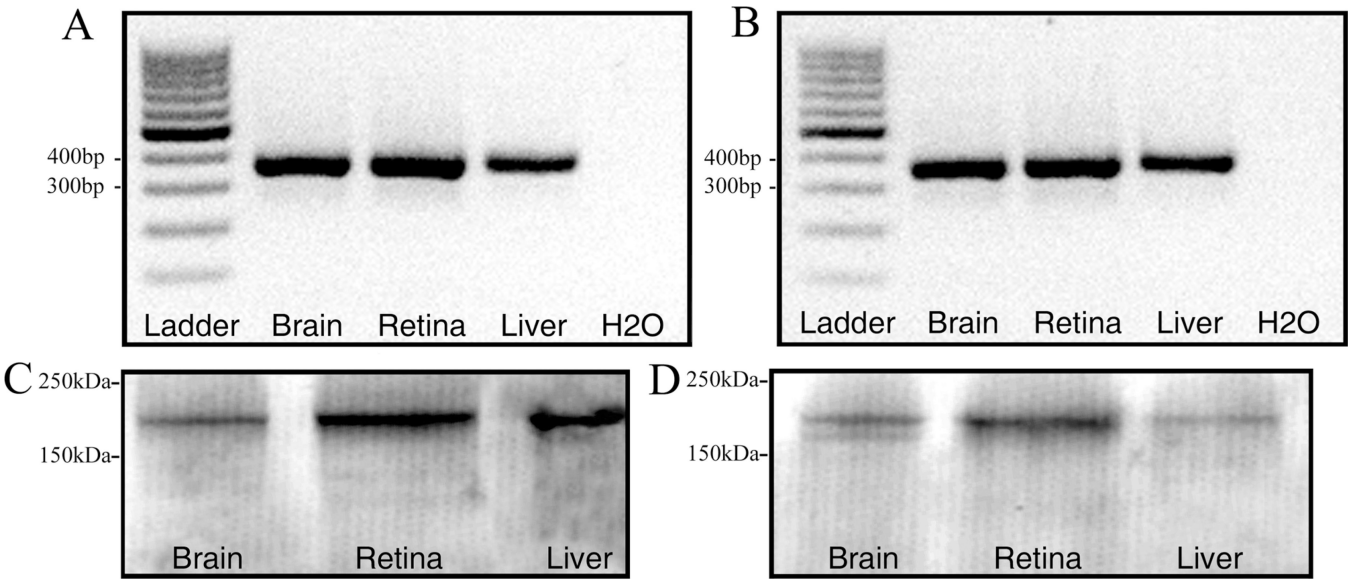

Figure 1.

Expression of $\alpha_2\delta_4$ subunit mRNA and protein. RT-PCR of $\alpha_2\delta_4$ subunit primer set (2) in rat (A) and mouse (B). A band of ~357 bp was amplified from the mouse and rat brain, retina, and liver. Lane L: 100-bp DNA ladder; lane 1: brain; lane 2: retina; lane 3: liver; ane 4: water. Characterization of $\alpha_2\delta_4$ subunit antibody by western blot in the brain, retina, and liver of rat (C) and mouse (D). A protein band of ~170 kDa was detected in these tissues. Lane 1: brain; lane 2: retina; lane 3: liver. A total protein of 35 lg per lane was loaded for the $\alpha_2\delta$ subunit immunoblots.

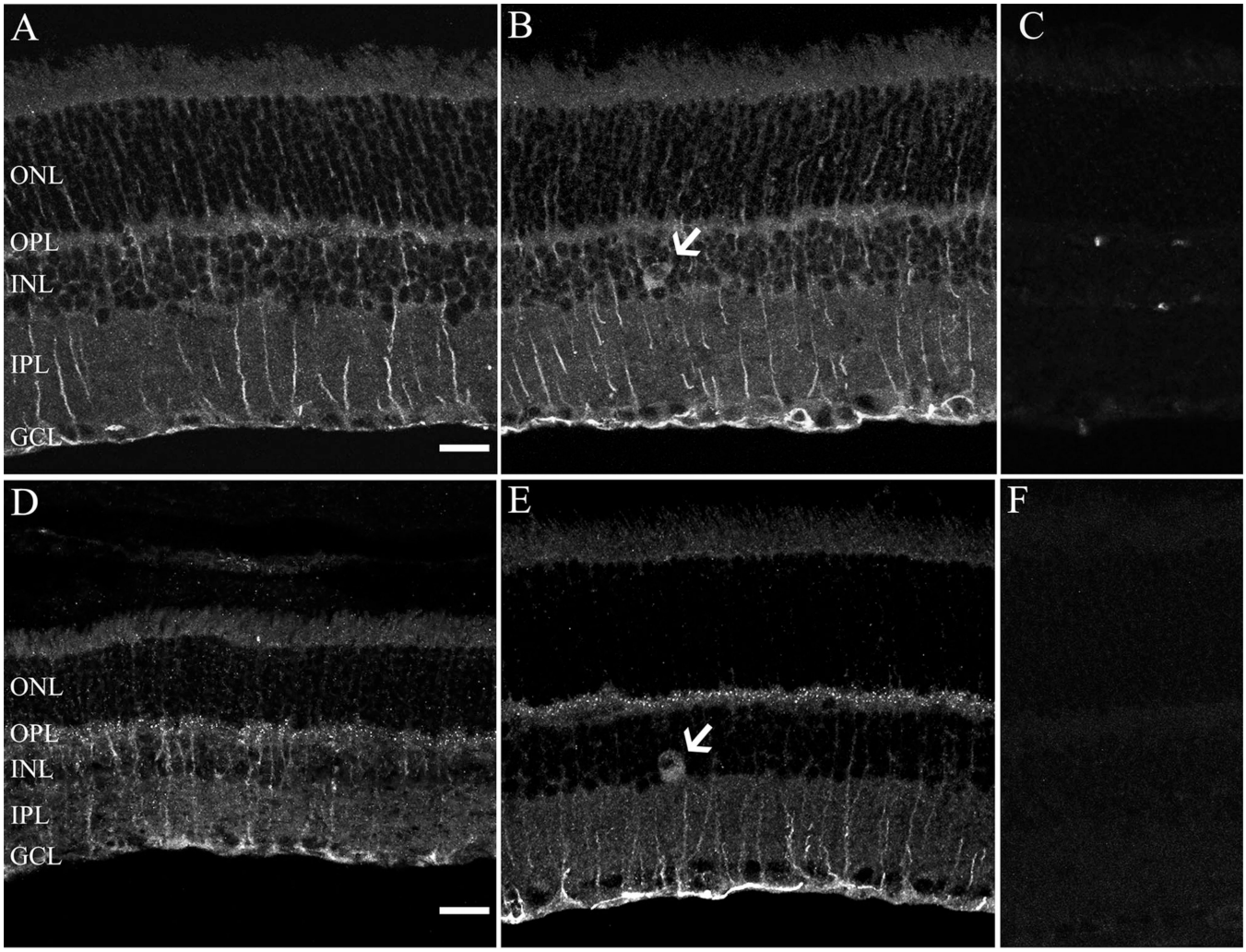

Figure 2.

Localization of $\alpha_2\delta_4$ subunit immunoreactivity in the rodent retina. $\alpha_2\delta_4$ subunit immunostaining was present in Mu¨ller cells, large cell bodies in the inner nuclear layer (INL) (arrow) and the outer plexiform layer (**OPL**) in rat (**A,B**) and mouse (**D,E**). Note that the im-munostaining in the OPL was characterized by strong puncta in the mouse retina. Retinal sections incubated with antibodies preadsorbed with the immunization peptide resulted in no specific staining in both rat (**C**) and mouse (**F**) retina. All micrographs are projections of 9–14 optical sections. GCL, ganglion cell layer; ONL, outer nuclear layer; IPL, inner plexiform layer. Scale bar = 20 μm in A (applies to A– C) and D (applies to D–F).

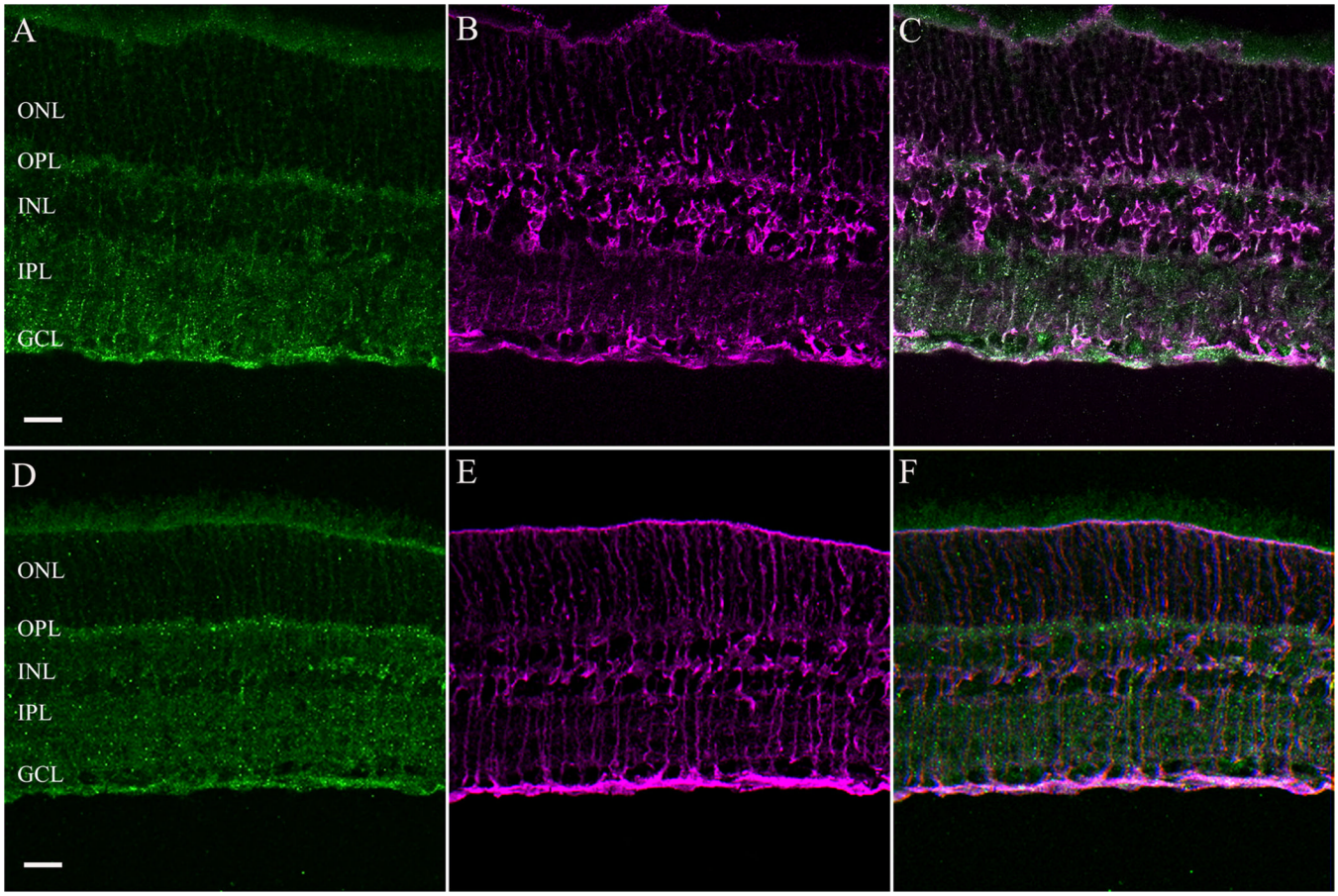

Figure 3.

Colocalization of the immunostaining for $\alpha_2\delta_4$ subunit (green) with glutamine synthetase (GS) (magenta), a marker for Müller cells in rat (**A–C**) and mouse (**D–F**) retina. GCL, ganglion cell layer; INL, inner nuclear layer; IPL, inner plexiform layer; ONL, outer nuclear layer; OPL, outer plexiform layer. Scale bar = 20 μm in A (applies to A–C) and D (applies to D–F).

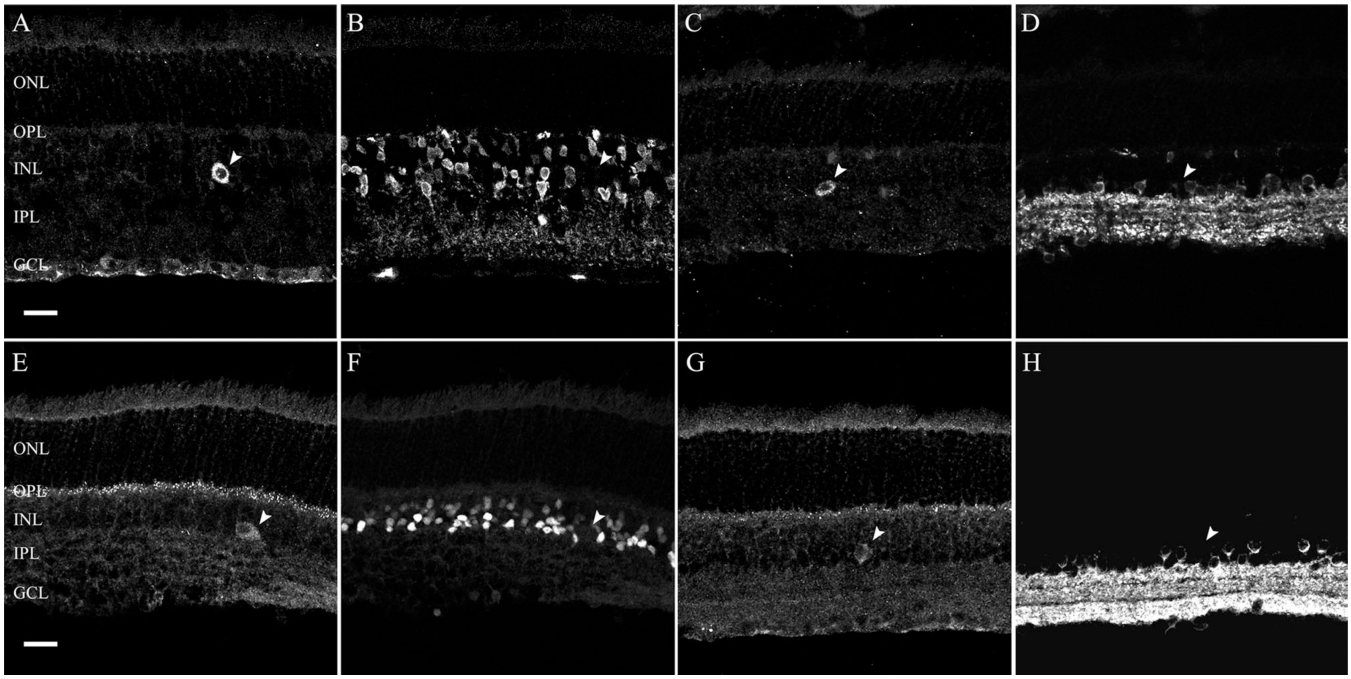

Figure 4.

$\alpha_2\delta_4$ subunit immunoreactivity is not present in glycine- and glutamic acid decarboxylase 65 and 67 (GAD_{65}/GAD_{67})-containing cells in the rodent retina. Glycine and GAD_{65}/GAD_{67} immunoreactivity are localized to amacrine cell bodies in the proximal INL. **A,B:** Single scan from a retinal section double labeled with $\alpha_2\delta_4$ subunit and glycine antibodies in the rat retina. A $\alpha_2\delta_4$ subunit-containing cell body (A; arrowhead) in the INL does not show glycine immunoreactivity (**B;** arrowhead). **C,D:** Single scan from a retinal section double labeled with $\alpha_2\delta_4$ and GAD antibodies in the rat retina. A $\alpha_2\delta_4$ subunit-containing cell body (C; arrowhead) in the INL does not show GAD immunoreactivity (D; arrowhead). **E,F:** Single scan from a retinal section double labeled with $\alpha_2\delta_4$ subunit and glycine antibodies in the mouse retina. A $\alpha_2\delta_4$ subunit containing cell body (E; arrowhead) in the INL does not have glycine immunoreactivity (F; arrowhead). G,H: Single scan from a retinal section double labeled with $\alpha_2\delta_4$ and GAD antibodies in the mouse retina. A $\alpha_2\delta_4$subunit-containing cell body (G; arrowhead) in the INL does not have GAD immunoreactivity (H; arrowhead). GCL, ganglion cell layer; INL, inner nuclear layer; IPL, inner plexiform layer; ONL, outer nuclear layer; OPL, outer plexiform layer. Scale bar = 20 lm in A (applies to A–D) and E (applies to E–H).

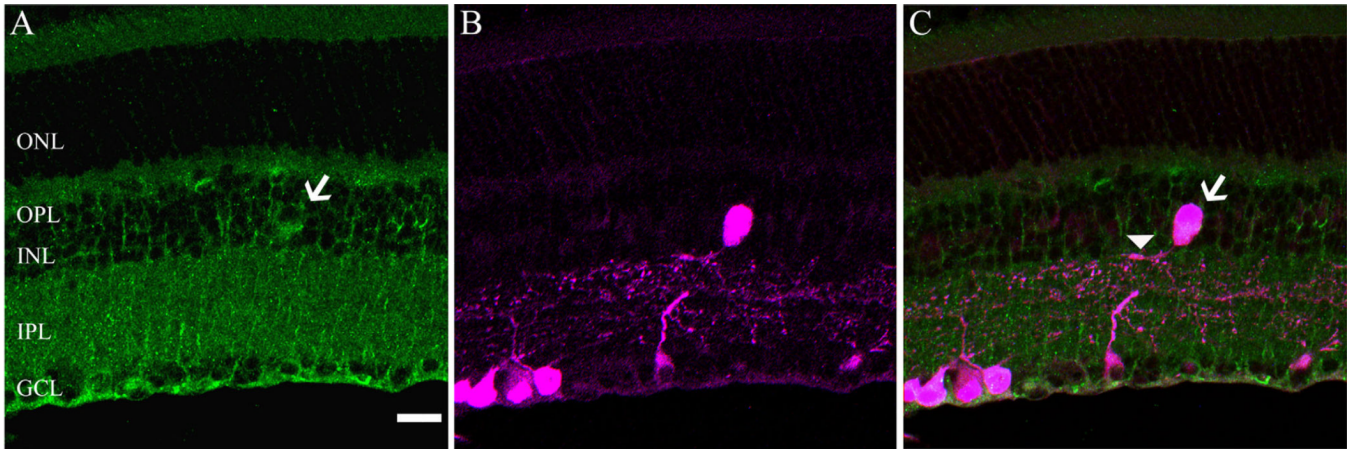

Figure 5.

Localization of the $\alpha_2\delta_4$ subunit in ganglion cells of a transgenic mouse line with tdTomato driven by the parvalbumin promoter. A: $\alpha_2\delta_4$ subunit immunostaining, showing a putative displaced ganglion cell. **B:** Transgenic mouse retina shows parvalbumin (PV) –tdTo-matoexpressing cells in the GCL and in the INL. **C:** Overlay demonstrating that the $\alpha_2\delta_4$subunit immunostained cell expresses PV-tdTo-mato in the INL (arrows). Note that the primary dendrites of the displaced ganglion cell are in the distal IPL corresponding to laminae 1–2 of the IPL (arrowhead), indicating that this cell is likely to be an OFF-type ganglion cell. GCL, ganglion cell layer; INL, inner nuclear layer; IPL, inner plexiform layer; ONL, outer nuclear layer; OPL, outer plexiform layer. Scale bar = 20 μm in A (applies to A–C).

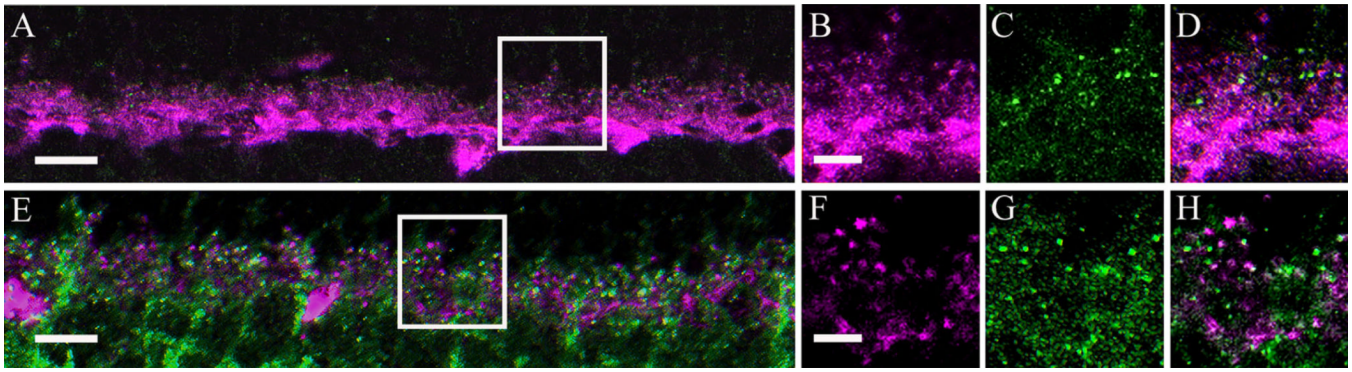

Figure 6.

$\alpha_2\delta_4$subunit immunoreactivity was not observed in horizontal cells or their processes in the mouse retina. **A:** Single scan showing horizontal cells identified with calbindin (magenta) immunostaining and the $\alpha_2\delta_4$ subunit immunostaining (green). **B–D:** High magnification (boxed area from A) of a single scan showing the $\alpha_2\delta_4$ subunit immunoreactivity (C), calbindin (B), and an overlay of the two, demonstrating a lack of colocalization (D). **E:** Single scan showing horizontal cells tips labeled with a VGAT (magenta) and $\alpha_2\delta_4$subunit antibody (green). **F–H:** High magnification (boxed area from E) of a single scan showing VGAT immunostaining (F), $\alpha_2\delta_4$ (G), and overlay (H).Scale bar = 20 μm in A,E; 2 μm in B (applies to B–D) and F (applies to F–H).

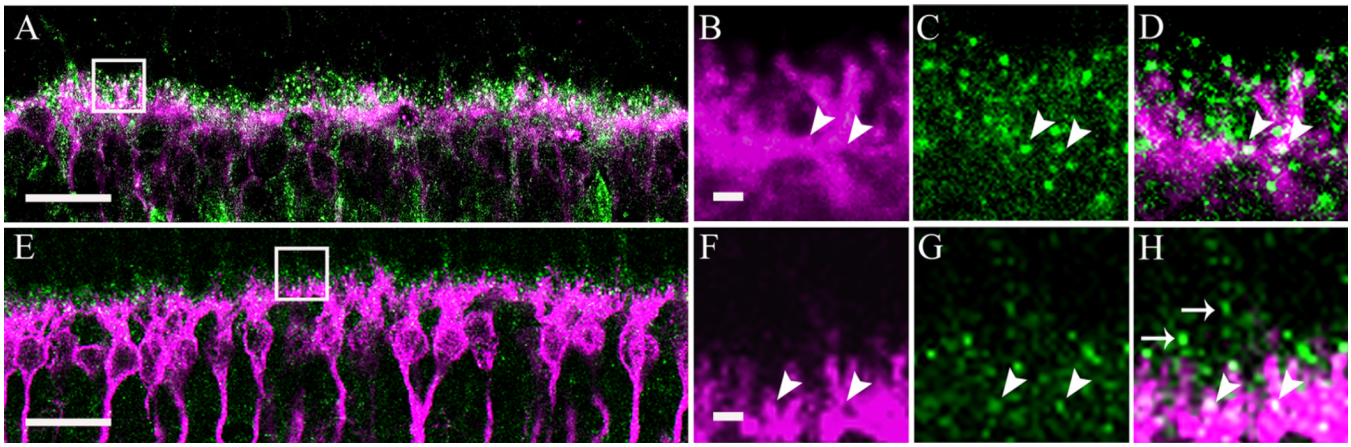

Figure 7.

$\alpha_2\delta_4$ subunit immunoreactivity was observed in ON-type bipolar cells identified by Goa or PKC immunostaining in the mouse retina. **A:** Goα immunoreactivity (magenta) and $\alpha_2\delta_4$ subunit immunoreactivity (green). **B–D:** High-magnification inset (boxed area from A) of a single scan showing colocalization of Goα and $\alpha_2\delta_4$ subunit immunoreactivities (arrowheads). **E:** PKC immunoreactivity (magenta) and $\alpha_2\delta_4$ subunit immunoreactivity (green). **F–H:** High-magnification inset (boxed area from E) of single scan showing colocalization of PKC and $\alpha_2\delta_4$ subunit immunoreactivities (arrowheads). Most of the $\alpha_2\delta_4$ subunit immunoreactive puncta are located in the upper part of the OPL (arrows) and are likely to be localized to photoreceptor terminals. Scale bar = 10 lm in A,E; 2 μm in B (applies to B–D) and F (applies to F–H).

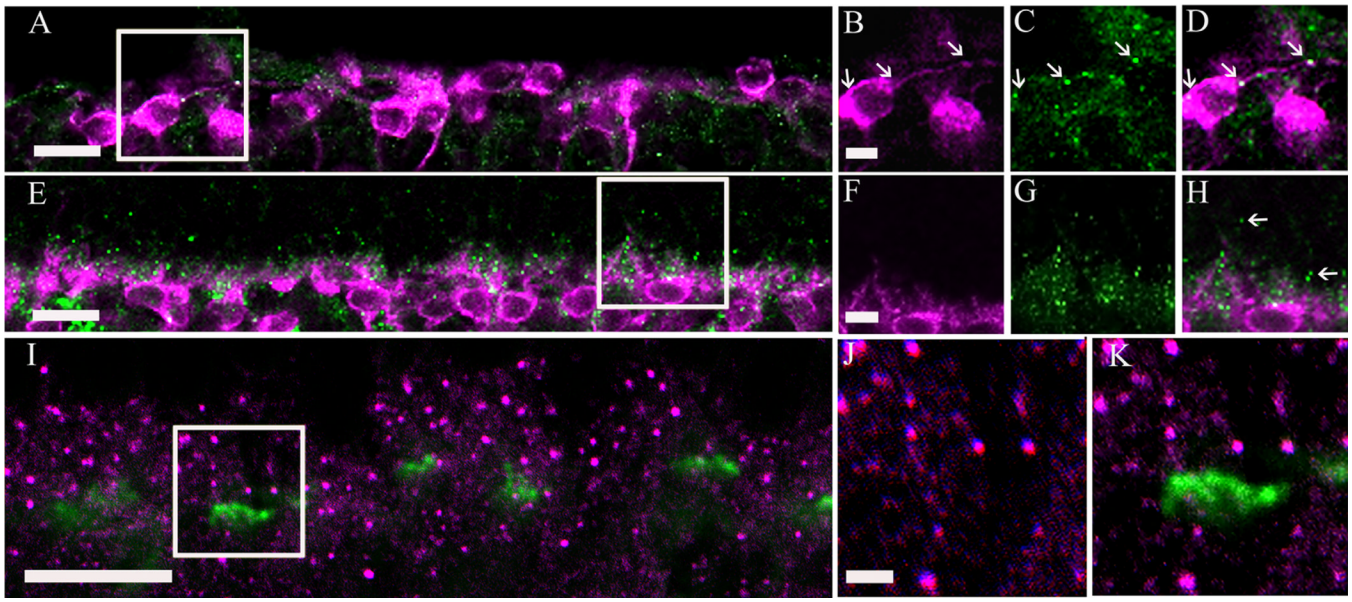

Figure 8.

$\alpha_2\delta_4$ subunit immunoreactivity was observed in photoreceptor terminals of the mouse retina. **A:** $\alpha_2\delta_4$ subunit and protein kinase C (PKC) immunoreactivity in a rd/rd adult mouse retina that lacks photoreceptors (Carter-Dawson et al., 1978). **B–D:** High-magnification view of a single scan (boxed area from A). $\alpha_2\delta_4$ subunit immunoreactivity was significantly reduced in the rd/rd adult mouse OPL and some of the remaining $\alpha_2\delta_4$ subunit immunoreactive puncta (green) colocalized with rod bipolar cell terminals (arrows) immunostained with PKC antibodies (magenta). **E:** $\alpha_2\delta_4$ subunit and PKC immunoreactivity in cone-DTA mice. These mice lack cone photoreceptors (Soucy et al., 1998). **F–H:** High-magnification view of single scan (boxed area from E) showing $\alpha_2\delta_4$ subunit immunoreactive puncta distal to rod bipolar cell dendrites (arrows) suggesting the presence of the $\alpha_2\delta_4$ subunit at rod photoreceptor terminals. **I:** Labeling of cone pedicles with peanut agglutinin (PNA) conjugated to FITC (green) and $\alpha_2\delta_4$ subunit antibody (magenta) in the wild-type mouse. **J,K:** High-magnification view of single scan showing that $\alpha_2\delta_4$ subunit immunoreactivity is not located at the base of cone pedicles. Scale bar = 10 μm in A,E,I; 2 μm in B (applies to B–D), F (applies to F–H), and J (applies to J,K).

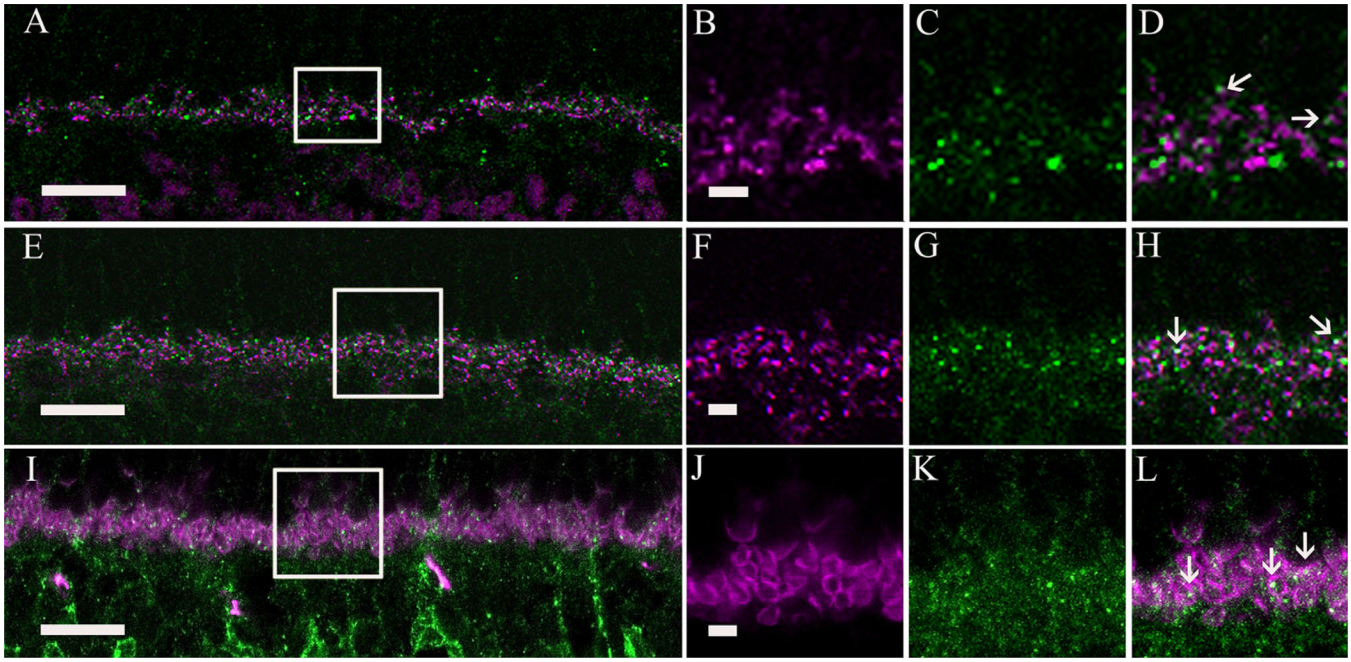

Figure 9.

Localization of $\alpha_2\delta_4$ subunit immunoreactivity in photoreceptor synapses in the mouse retina. **A:** Double immunolabeling of the $\alpha_2\delta_4$ subunit (green) and C-terminal binding protein 2 (CtBP2) (magenta), a synaptic ribbon marker. **B–D:** High-magnification view (boxed area from A) showing that $\alpha_2\delta_4$ subunit puncta do not colocalize with CtBP2 immunoreactivity (arrows). **E:** Double immunolabeling of the $\alpha_2\delta_4$ subunit (green) and bassoon (magenta), a photoreceptor presynaptic protein. **F–H:** High magnification (boxed area from E) showing overlap of $\alpha_2\delta_4$ subunit puncta with some of the bassoon immunoreactive profiles (arrows). **I:** Double immunolabeling of $\alpha_2\delta_4$ subunit (green) and postsynaptic density protein 95 (PSD-95) (magenta) in a wild-type mouse retina. **J–L:** High-magnification view (boxed area from I) showing that $\alpha_2\delta_4$ immunoreactive puncta were distributed inside the photoreceptor terminals. Scale bar = 10 μm in A,E,I; 2 lm in B (applies to B–D), F (applies to f–H), and J (applies to J–L).

TABLE 1

Primary Antibodies Used in This Study

Antibody	Antigen/immunogen	Species/dilution	Source/cat. no.
$\alpha_2\delta_4$	Calcium channel, voltage-dependent, α-2/δ subunit 4 recombinant protein epitope signature tag (PrEST). The antibody corresponds to human residues 324–401 of the Cacna2d4 protein. Immunogen sequence NDFINIIAYNDYVHYIEPCFKGILVQADRD NREHFKLLVEELMVKGVGVVDQALREAFQILKQFQEAKQGSLCNQAIM.	Rabbit polyclonal 1:100–1:500	Sigma, HPA031952
Bassoon	Recombinant rat Bassoon	Mouse 1:500	Life Science, SAP7F407
CtBP2	C-terminal binding protein-2 from mouse (361–445)	Mouse 1:10,000	BD Bioscience, 612044
GAD65	Purified rat brain glutamic acid decarboxylase	Mouse 1:1,000	Chemicon, MAB351
GAD67	Amino acid residues 4–101 of human GAD67	Mouse 1:1,000	Millipore, MAB5406
Glutamine synthetase	Sheep glutamine synthetase amino acids 1–373	Mouse 1:1,000	BD Biosciences, 610518
Glycine	Glycine paraformaldehyde conjugated to thyroglobulin	Rat polyclonal 1:1,000	D. Pow, University of Queensland, Australia
Goα	Purified Goα from bovine brain	Mouse 1:5,000	Millipore, MAB3073
PSD-95	Recombinant rat PSD-95	Mouse 1:1000	Millipore, MAB1596
Peanut agglutinin (PNA)	No immunogen; binds to galactosyl (b-1,3) N-acetylgalactosamine, fluorescein labeled	300 μg/ml	Vector, FL-1071
PKC	Hinge region of the calcium activated, phospholipid dependent protein kinase C from bovine brain; clone MC5	Mouse 1:1,000	Biodesign International, ME K01107M
VGAT	Synthetic peptide AEPPVEGDIHYQR (amino acids 75–87 in rat) coupled to keyhole limpet hemocyanin via an added N- terminal cysteine.	Mouse 1:1,000	Synaptic Systems, 131 011